

**ENDOTOXIN INFUSION IN RATS INDUCES APOPTOTIC AND SURVIVAL
PATHWAYS IN THE HEART**

By

Treena E. McDonald

B.Sc., University of Victoria, 1997

A THESIS SUBMITTED IN PARTIAL FULFILMENT OF THE REQUIREMENTS FOR THE
DEGREE OF
MASTER OF SCIENCE
IN
THE FACULTY OF GRADUATE STUDIES
DEPARTMENT OF EXPERIMENTAL MEDICINE

We accept this thesis as conforming to the required standard

THE UNIVERSITY OF BRITISH COLUMBIA

June 2000

©Treena E. McDonald, 2000

In presenting this thesis in partial fulfilment of the requirements for an advanced degree at the University of British Columbia, I agree that the Library shall make it freely available for reference and study. I further agree that permission for extensive copying of this thesis for scholarly purposes may be granted by the head of my department or by his or her representatives. It is understood that copying or publication of this thesis for financial gain shall not be allowed without my written permission.

Department of Experimental Medicine

The University of British Columbia
Vancouver, Canada

Date June 23, 2000

ABSTRACT

Inflammatory mediators of sepsis induce apoptosis in many cell lines. We tested the hypothesis that lipopolysaccharide (LPS) injection in vivo results in induction of early apoptotic and survival pathways as well as evidence of late-stage apoptosis in the heart. Hearts were collected from control rats and at 6, 12 and 24 hours after LPS injection (4 mg/kg). After LPS injection Bax (early pro-apoptotic) mRNA increased (16% at 24 hours, $p<0.05$) whereas Bax protein initially decreased (35% at 6 hours, $p<0.05$) and then returned to baseline values by 24 hours. Six hours after LPS injection Bcl-2 (early survival) mRNA levels increased while its protein levels decreased (70%, $p<0.05$) and then returned to baseline levels by 24 hours. Mitochondrial cytochrome C levels decreased suggestive of mitochondrial involvement. Activation of an apoptotic pathway was confirmed by the 1000 fold increase in caspase 3 activity at 24 hours ($p<0.05$). TUNEL staining identified myocardial cells undergoing DNA fragmentation with significant levels occurring at 24 hours post LPS injection. Heart function in this model as measured by myocyte contractility, showed a 29% decrease in fractional shortening at 6 hours after LPS injection with a 50% improvement present by 12 hours. Heart function at 24 hours was comparable to the 12 hour time point. Thus, activation of apoptotic and survival pathways in the heart occurs during a septic inflammatory response. The presence of apoptotic pathways temporarily correlates with myocardial dysfunction.

TABLE OF CONTENTS

| | |
|---------------|----|
| ABSTRACT..... | ii |
|---------------|----|

| | |
|----------------------|----|
| LIST OF TABLES | vi |
|----------------------|----|

| | |
|-----------------------|-----|
| LIST OF FIGURES | vii |
|-----------------------|-----|

| | |
|------------------------|------|
| ACKNOWLEDGEMENTS. | viii |
|------------------------|------|

CHAPTER 1: INTRODUCTION

| | |
|--|----|
| 1.1 Background of Sepsis | 1 |
| 1.2 Septic Myocardial Dysfunction | 2 |
| 1.3 General Features of Apoptosis | 6 |
| 1.4 Apoptosis and its Relationship to Sepsis Including Myocardial Dysfunction | 9 |
| 1.5 Hypothesis | 11 |
| 1.6 Experimental Approach | 11 |

CHAPTER 2: METHODS

| | |
|------------------------------|----|
| 2.1 Septic Rat Model | 18 |
| 2.2 RNA Isolation | 18 |
| 2.3 RT-PCR | 19 |
| 2.4 Protein Isolation | 20 |
| 2.5 Isolation of Bcl-2 | 21 |

| | | |
|------|--|----|
| 2.6 | Protein Analysis | 21 |
| 2.7 | Caspase 3 Activity Assay | 22 |
| 2.8 | TUNEL Staining | 23 |
| 2.9 | Isolation of Cardiac Myocytes | 23 |
| 2.10 | <i>In vitro</i> Challenge of Isolated Cardiac Myocytes..... | 24 |
| 2.11 | Measurements of Cardiac Myocyte Contractile Function | 25 |
| 2.12 | Morphology Analysis of <i>In Vitro</i> Challenged Cardiac Myocytes | 26 |
| 2.13 | Cell Fractionation | 26 |
| 2.14 | Statistical Analysis | 27 |

CHAPTER 3: RESULTS

| | | |
|-----|----------------------|----|
| 3.1 | In Vivo Model | 28 |
| 3.2 | In Vitro Model | 31 |

CHAPTER 4: DISCUSSION

| | | |
|-----|---|----|
| 4.1 | Summary of Main Findings | 43 |
| 4.2 | Bax versus Bcl-2 in the LPS Rat Model | 44 |
| 4.3 | Are Mitochondria Involved in LPS Induced Cardiac Apoptosis? | 48 |
| 4.4 | A Minimum of One Apoptotic Pathway was Activated in the LPS-Treated Heart | 53 |
| 4.5 | Presence of End-Stage Apoptosis in the LPS-Treated Heart | 56 |
| 4.6 | Comparison of Our Apoptotic and Survival Findings with Other Cardiac Models Related to Sepsis | 58 |
| 4.7 | Myocardial Function in the LPS-Treated Rat Model..... | 62 |

| | | |
|-----------------------------|--|----|
| 4.8 | In Vitro Analysis of Cardiac Myocytes for Investigating the Link Between Apoptosis and Cardiac Dysfunction | 66 |
| 4.9 | Pitfalls and Future Directions | 70 |
| 4.10 | Conclusions | 72 |
| CHAPTER 5: REFERENCES | | 73 |

LIST OF TABLES

| | |
|--|----|
| Table 1: TUNEL Analysis in the LPS-exposed Heart | 41 |
| Table 2: In <i>Vitro</i> Challenge of Cardiac Myocytes with Apoptosis Inducing Agents..... | 42 |

LIST OF FIGURES

| | |
|--|----|
| Figure 1: Mechanism of myocyte contractility | 13 |
| Figure 2: Apoptotic Pathways | 14 |
| Figure 3: A hypothetical scenario for the correlation between apoptosis and myocardial dysfunction | 15 |
| Figure 4: In Vivo Experimental Design | 16 |
| Figure 5: In Vitro Experimental Design | 17 |
| Figure 6: Bax Profile in the LPS-exposed Heart | 32 |
| Figure 7: Bcl-2 Profile in the LPS-exposed Heart..... | 33 |
| Figure 8: Bax/Bcl-2 Ratio | 34 |
| Figure 9: Cytochrome C Profile in the LPS-exposed Heart | 35 |
| Figure 10: Caspase 3 Profile in the LPS-exposed Heart | 36 |
| Figure 11: TUNEL Analysis in the LPS-exposed Heart | 37 |
| Figure 12: Fractional Shortening of Cardiac Myocytes Isolated from an LPS-exposed Heart | 38 |
| Figure 13: TNF α Effect on In Vitro Challenged Cardiac Myocytes | 39 |
| Figure 14: TNF α Effect on adult cardiac myocyte survival as determined by Morphology | 40 |

ACKNOWLEDGEMENTS

This work was supported by the Heart and Stroke Foundation of British Columbia and Yukon.

I would like to express my sincere thanks to Dr. Keith Walley for supervising this thesis. His ability to dive into a project has made this an exciting experience. I sincerely thank him for all his constructive criticism, helpful suggestions, and patience that has allowed me to reach my potential.

I would also like to thank Chris Carthy for performing the caspase 3 activity assay.

None of this would have been possible without the love and support from Paul McDonald.

CHAPTER 1: INTRODUCTION

1.1 Background of Sepsis

Sepsis affects 1%-2% of all hospitalized patients resulting in approximately 40 000 cases annually within Canada. Sepsis is also accompanied by a 20% to 30% mortality rate ^{1,2}. Sepsis develops as a secondary infection to the systemic presence of bacteria or fungi that have arisen from such illnesses as urinary tract and respiratory infections ¹. Most commonly, the infection is the result of either gram positive or gram negative bacteria ^{1,3}. Clinically, sepsis is defined and diagnosed as a patient with the following symptoms: positive blood culture for pathogens, fever or hypothermia, tachypnea, tachycardia, and one of the following: acidic blood, decreased urine output, hypotension, or deteriorated mental status ^{1,3}. Septic patients also suffer from a systemic inflammatory response, altered organ perfusion, and activation of both complement and coagulation cascades ^{1,4-6}. Many inflammatory cytokines are produced as a result of sepsis including tumor necrosis factor alpha (TNF α), interleukin-1 beta (IL-1 β), IL-2, IL-6, IL-8, IL-10, and interferon gamma (IFN- γ) ^{7,8}. TNF α and IL-1 β are among the first cytokines produced which further activate production of other inflammatory cytokines, nitric oxide and reactive oxygen intermediates (ROI). The levels of these cytokines and mediators can have detrimental effects as will be discussed through out this paper.

An alarming trend seen in the last few decades is a rise in the number of septic cases ^{2,3,9}. It is believed that this increase is contributed to by the use of immunosuppressive drugs and invasive medical procedures ^{3,10}. As well, the number of gram positive septic

cases has been increasing⁹. Current therapeutic approaches include antibiotics, surgery to remove dead tissue, fluid therapy, and vasoactive drugs^{9,10}. More novel therapies include antibodies directed against the gram negative bacteria, specifically to the lipid A domain of the lipopolysaccharide (LPS)^{11,12}. Other therapies include antibodies to pro-inflammatory cytokines (TNF α , IL-1 β)^{10,13,14}. However, these novel therapies show minimal success with regards to the disease profile and showed no effect on 28 day mortality rate¹¹⁻¹³.

Current mortality rates for sepsis are 20%-30% and rise to 60%-80% if cardiac dysfunction occurs as it does in 40% of all septic cases^{1,2,15}.

1.2 Septic Myocardial Dysfunction

Cardiac dysfunction in sepsis occurs due to a decrease in cardiac output¹⁶. Two contributing factors include alterations in systolic and diastolic function of the heart. Systolic function is depressed during sepsis despite a lower mean arterial pressure. This is accompanied by a decreased ejection fraction¹⁶. Survivors of sepsis, unlike non-survivors, compensate for this malfunction by dilating their left ventricle resulting in a return to a normal ejection fraction by day 6¹⁶. This lack of ventricular dilation (diastolic dysfunction) and decreased systolic function (systolic dysfunction) is believed to be the result of a circulating myocardial depressant^{15,16}.

Evidence for a circulating myocardial depressant factor (CMDf) comes from a variety of studies. Studies investigating the effect of septic serum on cultured cardiac myocytes have shown that the septic serum depresses cardiac contractility and frequency of contraction compared with control serum ¹⁷. No differences on cardiac function were detected between survivors and non-survivors of sepsis, implying that the CMDf was present in both populations irrespective of outcome ¹⁷. Dialysis of the serum prior to incubation with the myocytes resulted in the loss of the depressant activity. By the use of dialysis and gel filtration the molecular weight of the CMDf was determined to be approximately 2000 molecular weight ¹⁷. Similar evidence has been identified in animal studies. Sera from endotoxemic rats in the acute phase of the infection (1-3 hours post endotoxin injection) produced depressed cardiac function on *in vitro* myocytes ¹⁸. This early onset of myocardial dysfunction potentially suggests the negative influence of pro-inflammatory cytokines. Endotoxin had no direct cardiac myocyte depressant activity ¹⁸. Carli and colleagues also isolated and identified the depressant factor as being lipid soluble ¹⁸. Others have identified the myocardial depressant as water soluble ¹⁹. Thus a variety of CMDfs may be present.

Continued investigation into the CMDf has suggested that TNF α , IL-1 β , and other cytokines are all possibilities. Evidence includes the following. Characteristics of the CMDf had a similar profile to that of cytokines. Kumar and colleagues ²⁰ tested a variety of cytokines including IL-1 β , IL-2, IL-4, IL-6, IL-8, IL-10, IFN- γ , and TNF α for their effect on cultured myocytes. Only TNF α and IL-1 β showed any cardio depressant effects. As well, serum from patients with acute shock when pre-incubated with anti-

TNF α or anti- IL-1 β prior to incubation with cardiac myocytes resulted in an unaffected depressant activity but if both were immunoabsorbed then contractility was restored ²⁰. These studies suggest that TNF α and IL-1 β may have overlapping functions. Using anti-TNF α antibodies prior to induction of endotoxin in a septic pig model also showed improved Emax, a measurement of contractility, during the first four hours post injection ²¹. Blockage of TNF α , however, still showed a 10% depression in cardiac contractility ²¹ possibly the effect of IL-1 β . As well, TNF α challenged canines show a myocardial dysfunction similar to human septic shock characterized by a decreased ejection fraction, cardiac index, and mean arterial pressure ²². Ejection fraction can be affected by a variety of physiological responses including afterload, heart rate, and preload. Increased afterload and an increased heart rate decrease ejection fraction by decreasing stroke volume and filling time respectively. Increased preload results in an increased ejection fraction via the Starling Law mechanism. In a TNF α challenged canine model, the decrease in ejection fraction was not accounted for by changes in afterload, heart rate, or preload ²². In vitro studies of cardiac myocytes have also shown the cardiac depressant effect of TNF α , IL-2, and IL-6 mediated by nitric oxide (NO) ²³⁻²⁵. This finding is consistent with nitric oxide being a downstream respondent of TNF α . These studies stress the importance of TNF α , IL-1, and NO to trigger directly or indirectly myocardial dysfunction.

Myocyte contractility is shown in Figure 1. Two main requirements for cardiac myocyte contraction are ATP and calcium. Calcium regulation is controlled at multiple levels.

Calcium levels in the cytosol increase during systole as the result of extracting calcium from outside the cell via the L-type channel and release of calcium from the sarcoplasmic reticulum via the ryanodine receptor. To deplete the cytosol calcium concentration during diastole, calcium is extruded from the cell by the $\text{Na}^+ \text{-Ca}^{2+}$ exchange and by re-uptake by the sarcoplasmic reticulum. Calcium regulation is affected by sepsis ²⁶⁻²⁸. Calcium transport via the sarcoemmal vesicles is decreased during sepsis and the number of ryanodine receptors is less ^{26,28} thus not providing the calcium concentration necessary for full contraction. The $\text{Na}^+ \text{-Ca}^{2+}$ exchanger is less efficient making depletion of calcium from the cytosol during diastole difficult thereby not allowing full relaxation of the cardiac myocyte ²⁷. This disruption in calcium regulation results in a less dynamic change in calcium levels between systole and diastole thereby decreasing myocyte contraction. Two of the proposed CMDF, $\text{TNF}\alpha$ and nitric oxide, are known to interfere with calcium regulation. $\text{TNF}\alpha$ is thought to interfere with calcium regulation by inhibiting the calcium flux through the L-type channel, decreasing myofilament responsiveness to calcium, and by affecting cAMP production ²⁹ (Figure 1). Nitric oxide stimulates production of guanylate cyclase which reduces intracellular calcium and thereby decreases myocyte contractility ^{30,31}. Thus, part of the mechanism whereby $\text{TNF}\alpha$ and nitric oxide depress cardiac contractility is by interfering with the necessary calcium regulation. $\text{TNF}\alpha$ and NO may also cause cardiac dysfunction by other means. Therapeutic interventions have not been successful (see above), suggesting that unknown pathways and mechanisms of cardiac dysfunction have become activated prior to therapeutic intervention. Hence, the importance of determining downstream respondents of known CMDF. One such pathway may be the induction of apoptosis.

1.3 General features of Apoptosis

Characteristics Unique to Apoptosis

Until the 1970's necrosis was the only one form of cell death known³². In 1972 Kerr and colleagues identified an alternative mechanisms of cell death which was named apoptosis based on the Greek word for "falling off"³³. Necrosis occurs when a cell dies by "accident"³² as the result of a powerful insult such as ischemia, bacterial or viral infection, or lack of ATP production. Cells undergoing necrosis swell resulting in a loss of membrane integrity and the release of their cytosolic contents. Leakage of these internal contents causes neighboring cells to also die by necrosis and activate the immune system³⁴. Apoptosis, otherwise known as programmed cell death, is the result of cell suicide^{32,34}. The function of apoptosis is to remove unwanted cells, to counterbalance cell proliferation, and to help develop organ architecture. Every day examples of apoptosis include remodeling during fetal development and removal and clearance of aged leukocytes and normal sloughing of epithelial cells. Cells undergoing apoptosis present distinct and unique morphological features when the process is almost complete, which will be referred to as end-stage apoptosis. These characteristics include chromatin condensation resulting in the nucleus looking like a "half-moon", as well the cell shrinks in size, and the membrane blebs (seen only *in vitro*)³⁴. Another hallmark of apoptosis is that the DNA of the cell becomes cleaved at 180- 200 base pair intervals which appears as a "ladder" when electrophoresed on an agarose gel³⁴. Apoptotic cells do not activate the immune system, instead they are engulfed by phagocytic cells including macrophages/monocytes and by other nearby non-phagocytic cells such as vascular smooth muscle cells. It is believed that these phagocytic cells recognize a cell as being

apoptotic if there is an increase in the number of phosphatidylserine residues expressed on the cell's outer membrane ³⁴. The entire apoptotic process can occur within hours ³⁵.

Caspase/Bcl-2 Family

These morphometric markers of apoptosis are preceded by a number of conserved pathways. Some of these pathways are presented in Figure 2. Two main protein families, the caspases and the Bcl-2 family, have been shown to play an important role in determining the induction of apoptosis in a variety of cell types under a variety of conditions ³². Members of the caspase family contain a prodomain and an enzymatic domain ³². Caspases are present as an inert protein in the cell's cytosol until its enzymatic region is cleaved into a small and large subunit ³². The active caspase is composed of the 2 small and the 2 large subunits ³². Caspases cleave behind an aspartate residue, which also happens to be their own cleavage site. Thus caspases can activate other caspases. Caspases are considered to be “effector machinery” of apoptosis ³². Caspases have the ability to cleave nuclear proteins (laminin, PARP), regulatory proteins (DNA fragmentation factor, MEKK1), and cytoskeletal proteins (actin, gelsolin) ³². Caspase 3 can be activated by multiple apoptotic pathways including those of caspase origin, making it a junction point and an indicator of apoptotic activation. However, end-stage apoptosis can occur without activation of caspase 3. The role of the Bcl-2 family in apoptosis is regulatory ³². The Bcl-2 family includes both anti-apoptotic (Bcl-2, Bcl-xL, Mcl-1) and pro-apoptotic (Bax, Bad, Bid, Bcl-xs) proteins. Many Bcl-2 family members, except Bad and Bid, contain a transmembrane domain enabling them to localize to the outer mitochondrial and nuclear membranes and to the endoplasmic

reticulum ^{32,36}. Bcl-2 and Bax are the most studied proteins within the family. Bcl-2 residing on the mitochondria membrane prevents the release of cytochrome C, an event that can trigger caspase-3 activation. Bcl-2's role as an anti-apoptotic protein is countered by the pro-apoptotic Bcl-2 family members, especially Bax. Bcl-2 and Bax can form a heterodimer while Bcl-2 can form a homodimer ^{32,36}. The protein ratio of Bcl-2 to Bax has been shown as an important indicator of cell fate. A decrease in Bcl-2 is commonly accompanied by a rise in Bax in cells that ultimately progress to end-stage apoptosis ^{37,38}. Bcl-2 also exerts its pro-survival effect in the cardiac myocyte by activating an unidentified kinase(s) which is capable of phosphorylating I κ B causing the release of NF- κ B ³⁹. Bcl-2 increases mitochondrial buffering capacity of calcium and may regulate the pH of the intermembrane space ⁴⁰.

Bax resides in the cytosol until a death signal is received at which time the trans-membrane portion is exposed by inhibiting the actions of the amino terminal, allowing translocation to the mitochondria ⁴¹. Bax cytotoxicity is thought to be pH and voltage dependent ⁴⁰. The Bax gene can be transcriptionally regulated by the pro-apoptotic protein p53, which itself is activated in the presence of cleaved DNA ⁴². Bax mRNA can be downregulated by IL-6 ⁴². As one may have guessed from the location of the Bcl-2 family within the cell and its ability to promote or prevent release of other proteins from the mitochondria, the Bcl-2 family helps regulate the involvement of the mitochondria in the apoptotic process.

Mitochondria Involvement in Apoptosis

Mitochondria are frequently involved in the apoptosis process ^{40,43-45}. As indicated in Figure 3, mitochondria have the ability to release multiple proteins including cytochrome C, apoptosis inducing factor (AIF), caspase 2, pro-caspase 9, and DNase. Release of cytochrome C and apoptosis inducing factor ensure activation of the apoptotic pathway. Cytochrome C normally functions within the mitochondria as an electron chaperon between complex III (ubiquinol) and complex IV (cytochrome oxidase) ⁴³. Release of cytochrome C into the cytosol occurs with or without permeability transition pore (PT) opening and with or without a decreased mitochondria transmembrane electrical potential, $\Delta\Psi_m$ ^{45,46}. Once in the cytosol, cytochrome C can interact with dATP/ATP, pro-caspase 9, and APAF-1 to activate caspase 9. AIF can also be released through the PT pore of the mitochondria causing volume dysregulation which can result in apoptosis ⁴⁰. AIF and cytochrome C can induce release of each other thereby providing an overlap in apoptotic signaling ⁴³. The PT pore can be activated by caspases, oxidants, calcium ($>>10\ \mu\text{M}$), low ATP levels, reduced $\Delta\Psi_m$, ROI, nitric oxide, and by Bax ^{40,43-45,47}. The PT pore connects the inner and outer membranes of the mitochondria and participates in regulating matrix calcium, pH, $\Delta\Psi_m$, and volume ⁴⁵. Thus, mitochondria can be involved in inducing apoptosis.

1.4 Apoptosis and its Relation to Sepsis including Myocardial Dysfunction

Apoptosis is accelerated in some cells and delayed in others during sepsis. Accelerated apoptosis occurs in mucosal B-cells ⁴⁸, lymphocytes ^{49,50}, macrophages ^{51,52},

thymocytes ⁵³, hepatocytes ^{54,55}, and splenocytes ^{50,54}. PMN apoptosis on the other hand appears to be delayed during sepsis ^{56,57}.

The only report addressing heart apoptosis is from Hotchkiss and colleagues ⁵⁸. Apoptosis was found to be less than 1% and therefore was not investigated any further. The fraction of apoptotic cells within a healthy heart is reported to be ~0.001%. Thus, concluding that apoptosis does not increase in the septic heart with an apoptotic rate of less than 1% may not be correct. Thus the ability of cardiac myocytes to undergo apoptosis has not been fully investigated. Cardiac myocytes are unlike the above cell types in that they represent a terminally differentiated cell, and as such, apoptosis is uncommon because replacement is impossible. However, cardiac myocyte apoptosis has been documented during development as well as in disease states such as myocardial infarction, congestive heart failure, and ischemia reperfusion ⁵⁹⁻⁶². Cardiac myocyte apoptosis has been causally linked with age associated heart dysfunction ⁶³, and occurs in failing but not in non-failing ventricles of spontaneously hypertensive rats ⁶⁴. Thus, apoptotic pathways can be activated in cardiomyocytes under specific conditions. Conceivably apoptosis could occur during sepsis and inflammatory mediators could contribute. For example, TNF α has the ability to activate apoptotic pathways in many cell lines via TNF receptor type 1 (figure 2). TNF receptor type 1 is expressed on cardiac myocytes ³². Indeed, TNF α induces apoptosis in cardiac myocytes *in vitro* ⁶⁵. More recently, LPS challenged cardiac myocytes has been shown to induce apoptosis of these cells via myocyte induced TNF α release ⁶⁶. In addition, cytokine-stimulation of iNOS

resulting in nitric oxide production by the myocyte itself, by endothelial cells, and by leukocytes sequestered within the heart ^{67,68} may also contribute to apoptosis ^{69,70}. Thus, a number of mediators of sepsis could activate apoptotic pathways in the heart, although this has not been demonstrated *in vivo*.

1.5 Hypothesis

We hypothesize that during sepsis, apoptotic and survival pathways are activated in the heart and specifically within the cardiac myocyte. We further postulate that activation of these apoptotic pathways will be countered by regulatory pro-survival pathways resulting in minimum end-stage apoptosis. We also hypothesize that activation, but not completion of apoptotic pathways, may occur and that mitochondrial involvement in apoptotic pathways may contribute to the myocardial dysfunction present during sepsis (Figure 3).

1.6 Experimental Approach

Accordingly we propose to test this hypotheses by investigating apoptotic and survival pathways in the heart of an acute lipopolysaccharide (LPS) model of sepsis in male rats (Figure 4). Furthermore, the time course of activation of these apoptotic and survival pathways in the heart will be determined. Activation of pathways in this thesis refers to any change in mRNA, protein, or functional levels that occur as the result of endotoxin injection. We chose this terminology to reflect that the pathway is being activated upon whether in a positive or negative way. We have chosen to investigate the early pro-apoptotic protein, Bax; the early pro-survival protein, Bcl-2; and their downstream

effectors cytochrome C and caspase 3. Bax, Bcl-2, and caspase 3 will be investigated by measuring relative levels of their mRNA and protein expression. Cytochrome C will be investigated for its translocation from the mitochondria to the cytosol indicative of apoptosis. Caspase 3 enzymatic activity will also be measured. As well end-stage apoptosis will be investigated by TUNEL.

Part 2 of the study focuses on the connection between activation of apoptotic pathways and their role on myocardial dysfunction. To investigate this correlation, adult cardiac myocytes from healthy male Sprague Dawley rats will be isolated and cultured (Figure 5). The cultured myocytes will be treated with a variety of agents reported to cause end-stage apoptosis within 24 hours. These include $\text{TNF}\alpha$, IL-1 β , sphingosine, staurosporine, camptothecin, and Fas. After 24 hours of treatment the condition of the myocytes will be determined. Morphology, TUNEL, and fractional shortening will be performed to determine the status of the cell both with regards to survival as well as function. Once an end-stage apoptotic cardiac myocyte population can be established, the pathways involved and their timing will be investigated. The apoptotic pathways to be investigated include those studied in the *in vivo* study (Bax/Bcl-2, cytochrome C release, and caspase 3) plus additional analysis involving mitochondria membrane potential. Inhibitors (Figure 3) will then be used to block one or more of the activated apoptotic pathways to determine the effect on cardiac function, as measured by fractional shortening.

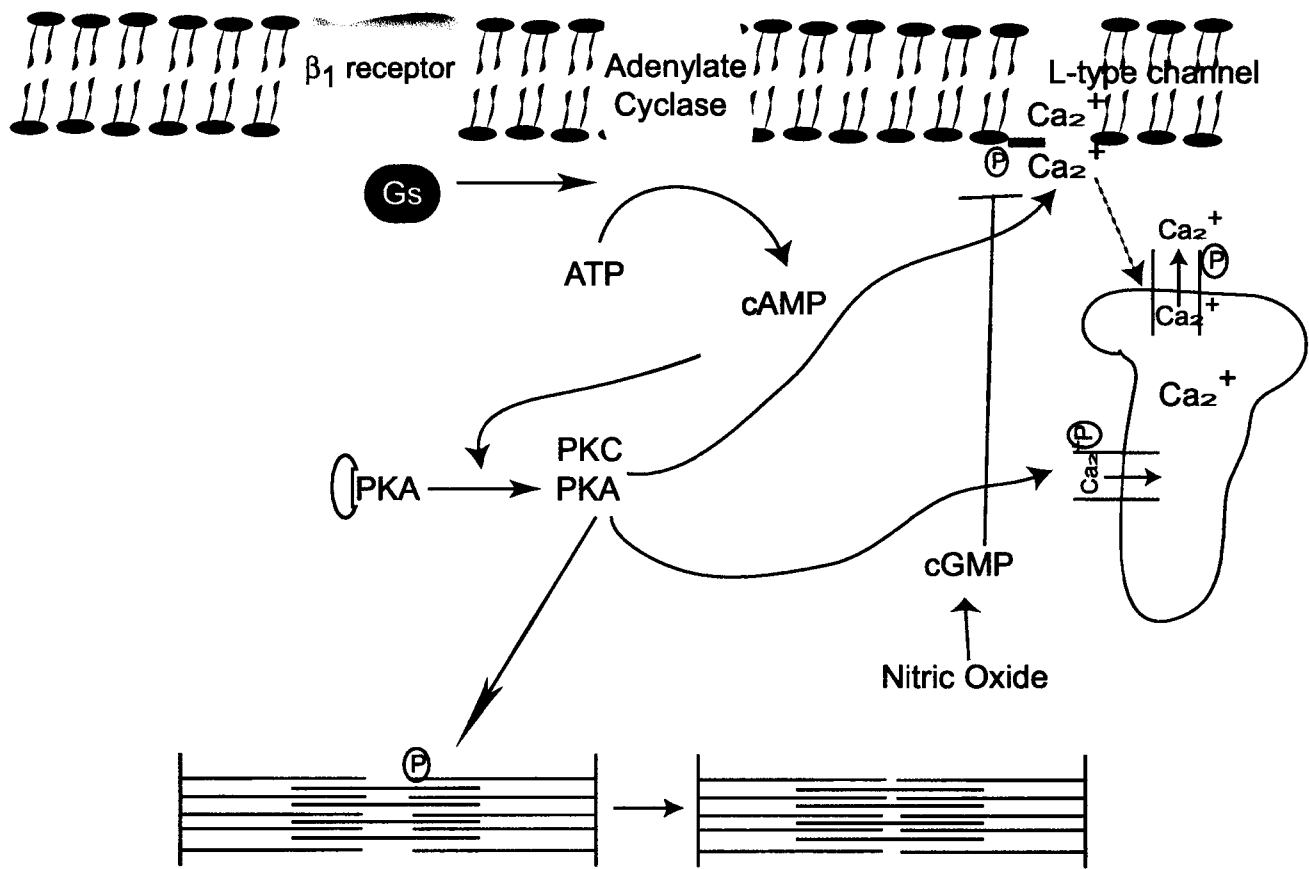


Figure 1: Mechanism of myocyte contractility. The β_1 receptor can be stimulated causing activation of cAMP followed by PKA activation. PKA increases myocyte contractility by opening the L-type channel thereby increasing calcium induced calcium release (CICR), by increasing the re-uptake of calcium by the sarcoplasmic reticulum, and by phosphorylating myosin to increase the rate of crossbridge cycling. PKC has similar functions to that of PKA but is not activated by cAMP. Nitric oxide has the opposite function and therefore decreases myocyte contractility. Nitric oxide exerts its effect by decreasing the time the L-type channel is opened thereby decreasing CICR.

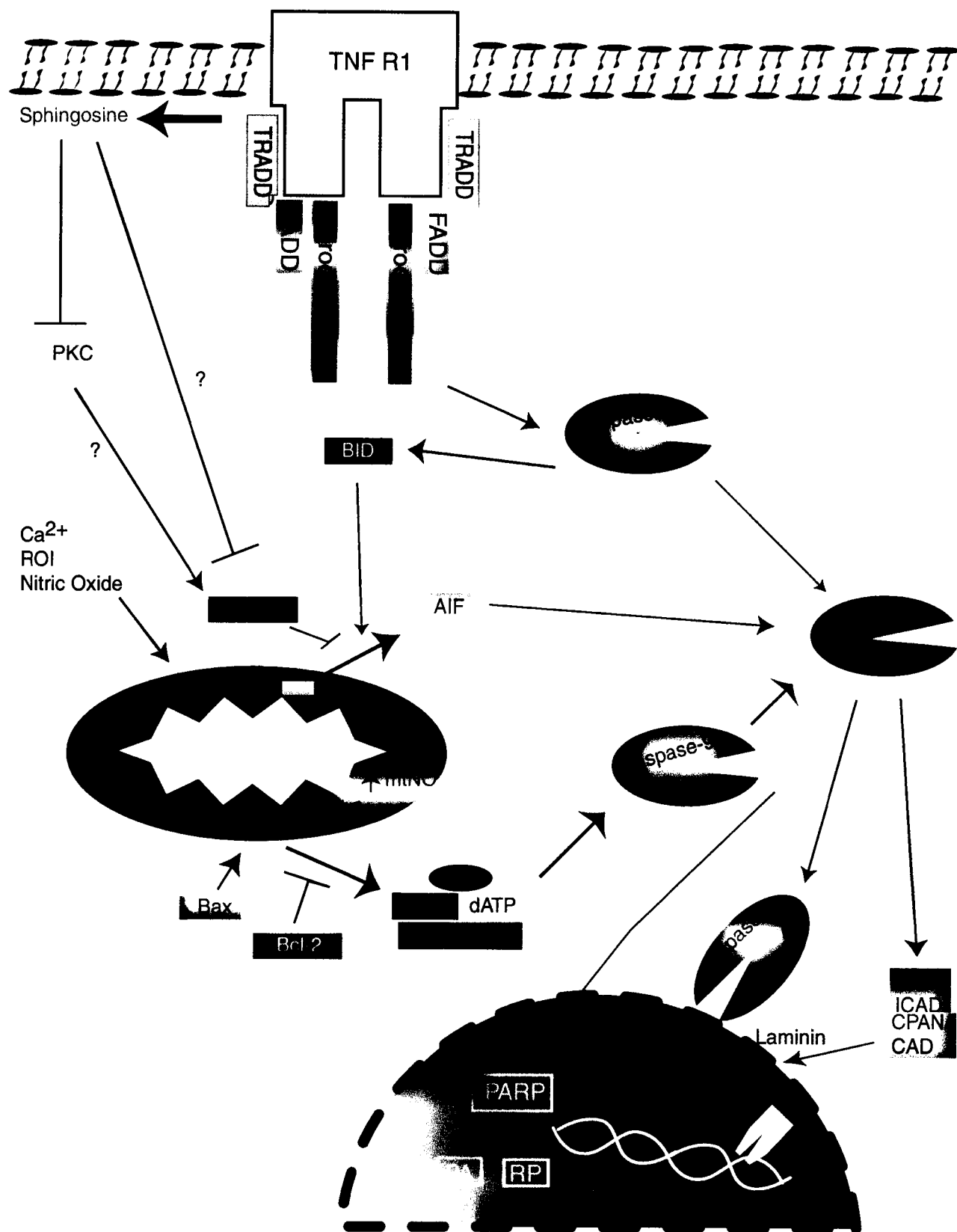


Figure 2. A schematic diagram representing potential apoptotic pathways activated in the LPS-exposed heart. The diagram is a modification of that presented by Granville and colleagues.

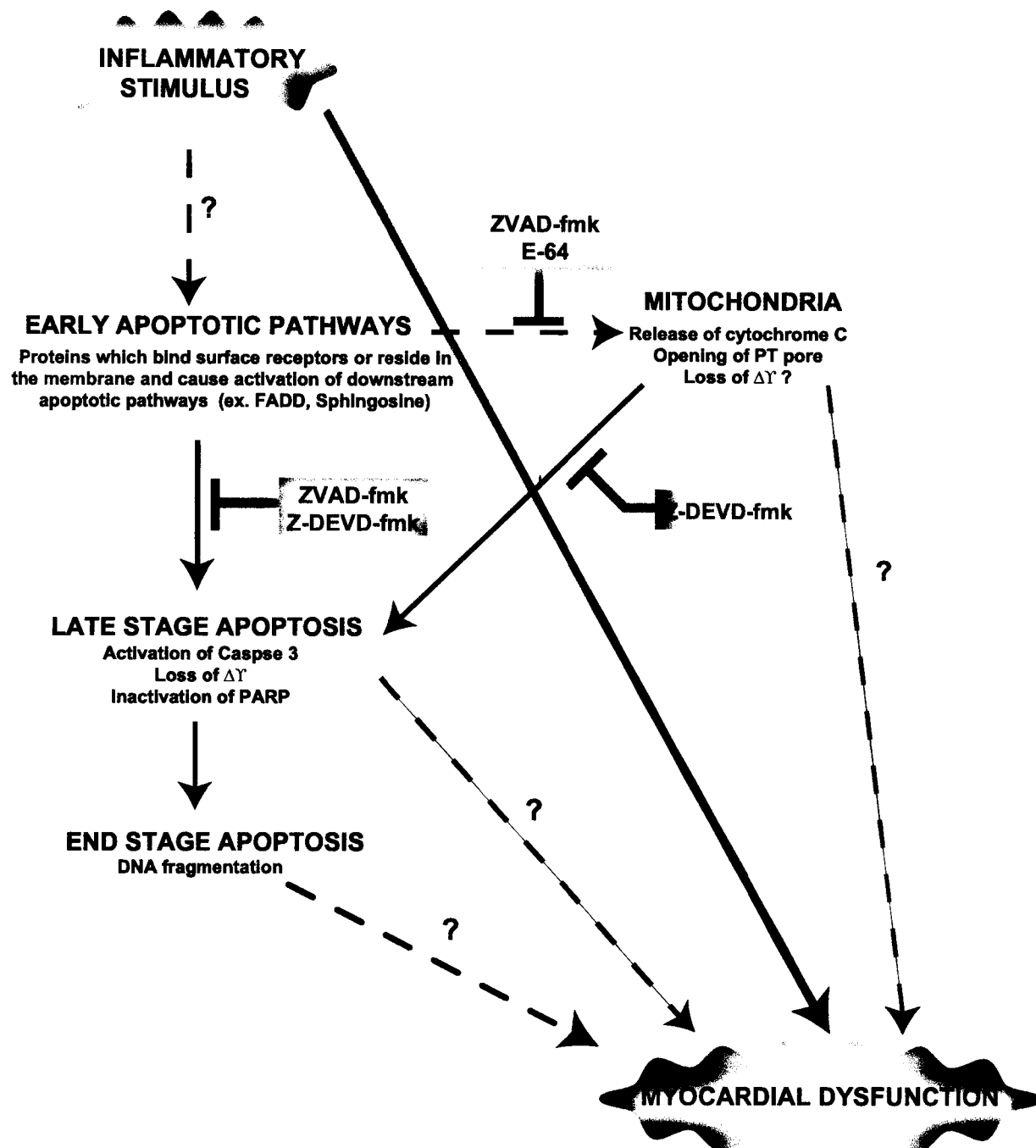


Figure 3. A schematic diagram of the hypothetical relationship between apoptosis and myocardial dysfunction.

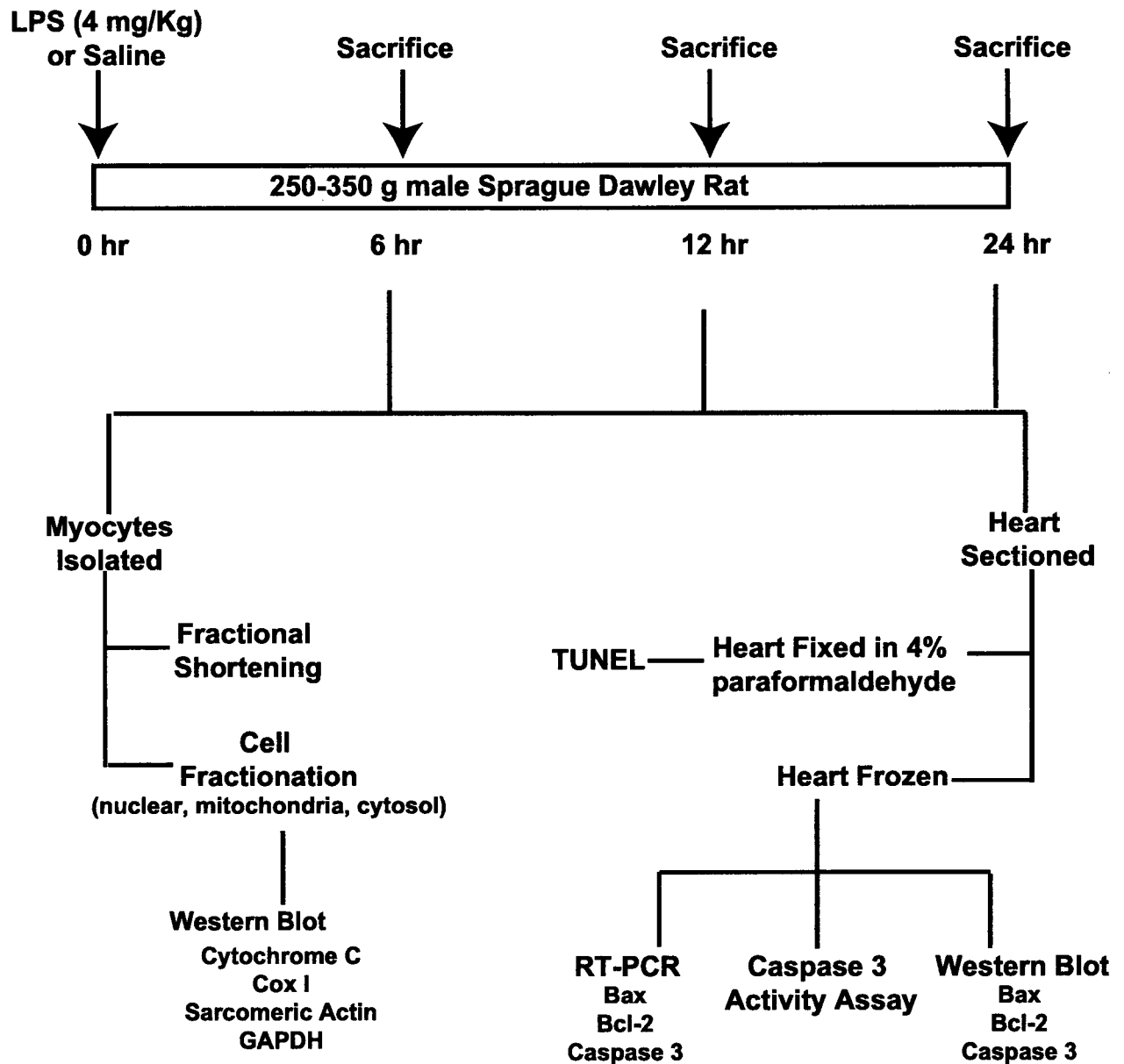


Figure 4. Experimental design for analyzing apoptosis in a LPS-Treated rat model.

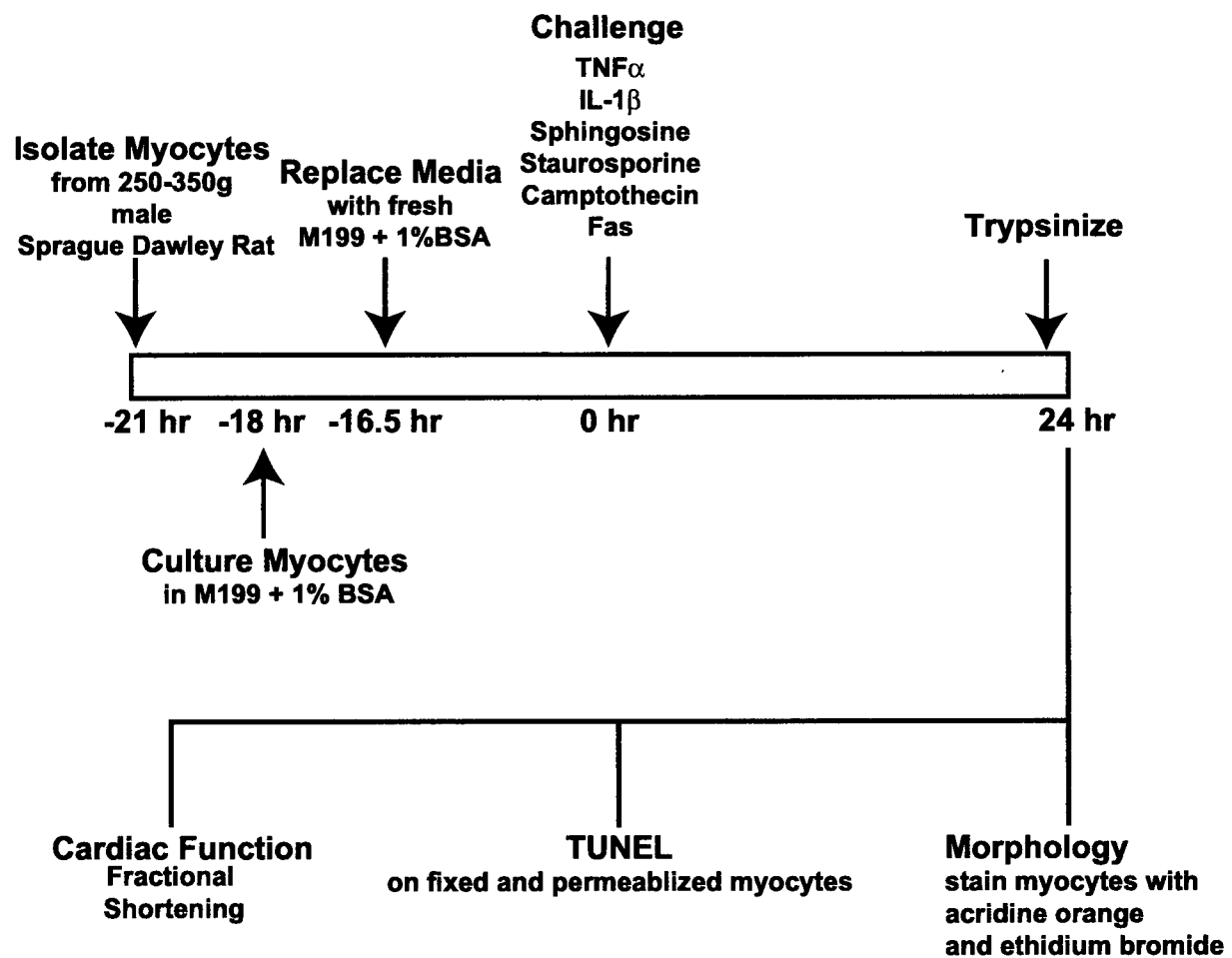


Figure 5. Experimental Design for Establishing an *in vitro* apoptotic cardiac myocyte population

CHAPTER 2: METHODS

2.1 Septic Rat Model

These experiments conform to NIH guidelines for the care and handling of animals and were approved by the University of British Columbia Animal Ethics Board. 250g – 350g male Sprague Dawley rats were given an intraperitoneal injection of 1 mL PBS or 4 mg/kg of LPS diluted in 1 mL PBS. Rats were sacrificed at multiple time points up to 24 hours post injection. Hearts were rapidly excised, cross-sectioned into 3-4 mm thick slices that included both right and left ventricle, and subsequently frozen in liquid nitrogen or fixed with 10% formalin. Frozen samples were stored at -80°C until needed and the fixed samples were paraffin embedded.

2.2 RNA Isolation

RNA was extracted from one section of each rat heart using phenol/chloroform. Briefly, the heart section was homogenized in RNase free nucleic acid extraction buffer and then phenol extraction buffer was added. RNA was isolated from this solution by a series of acid phenol:chloroform extractions. Finally the RNA was precipitated and resuspended in RNase-free water. Quantification of the RNA was performed using spectroscopy. RNA concentration in solution was then adjusted to 2.5 µg/µL.

2.3 RT-PCR

Five μg of RNA was reverse transcribed using 6 units of *SuperScript II reverse transcriptase* (Gibco BRL, Burlington Canada), 12.5 ng/ μL oligo [dT]₁₂₋₁₈ (Gibco BRL), and 500 μM of each dNTP (Gibco BRL), in a solution of 1 U RNasin (Promega, Madison WI), 5 μM DTT (Gibco BRL), and 1X buffer (50 mM Tris-HCl, pH 8.3; 75 mM KCl, 3 mM MgCl₂) in a total volume of 20 μL . The reaction was carried out at 37°C for 60 minutes followed by 95°C for 20 minutes in order to heat inactivate the reverse transcriptase.

Primers for Bax are 5' CCG AGA GGT CTT CTT CCG TGT G 3' and 5' GCC TCA GCC CAT CTT CTT CCA 3'; for Bcl-2 are 5'CAA GCC GGG AGA ACA GGG TA 3' and 5'CCC ACC GAA CTC AAA GAA GGC 3. Caspase 3 primers are 5' GGT ACC GAT GTC GAT GCA GCT 3' and 5' GGG TGC GGA AGA GTA AGC ATA 3'. PCR primers for GAPDH were taken from the literature and are 5' CCC ATC ACC ATC TTC CAG 3' and 5' ATG ACC TTG CCC ACA GCC 3'⁷¹. Reverse transcribed RNA (0.5 μg in 2 μL) was then mixed with 1 X PCR buffer (20 mM Tris-HCl, pH 8.4; 50 mM KCl); 1.0, 2.0, or 2.5 mM MgCl₂ for amplification of Bax , Bcl-2, or caspase 3 respectively; 20 μM of each dNTP, 20 ng/ μL of each primer set or 2.5 μM of each GAPDH primer, and 1 U *Taq* DNA polymerase (Gibco BRL) in a 20 μL reaction volume. The positive control consisted of rat lung cDNA. The negative control consisted of the PCR reaction mixture with no template added. GAPDH amplification was carried out with each gene of interest with its corresponding MgCl₂ concentration and specific thermal cycle program. PCR mixtures used the following conditions for Bax amplification: 38 cycles of 95°C for

30 seconds, 57.0°C for 40 seconds, 72°C for 25 seconds followed by one cycle of 72°C for 6 minutes. The PCR thermal cycle conditions for Bcl-2 and caspase 3 were identical to Bax with the following changes: the annealing temperature was respectively 61.2°C or 55.6 °C for 45 seconds, and the extension was for 30 seconds. PCR conditions were confirmed to be within the linear range for the respective cDNA amplification. PCR products were identified by electrophoresing 10 µL of the PCR mixture on a 2% agarose gel in TAE containing 0.2 µg of ethidium bromide per mL of gel. The resulting image was captured and densitometry performed using Eagle Eye™ (Stratagene, La Jolla CA). Densitometry results for the gene of interest were compared with corresponding GAPDH levels to account for loading differences. LPS did not alter GAPDH mRNA expression.

2.4 Protein Isolation

One frozen section from each rat heart was homogenized in ice-cold lysis buffer at a concentration of 0.5 g tissue/mL of lysis buffer. The homogenized sample was gently rotated for 30 minutes and subsequently sonicated and centrifuged at 10,000 g for 10 minutes with all steps being carried out at 4°C or on ice. The supernatant was collected and stored at -80°C. 50 µg of protein lysate was prepared in loading buffer (62.5 mM Tris-HCl pH 6.8, 10% (v/v) glycerol, 2% (w/v) SDS, 10% (v/v) 2-mercaptoethanol, 0.05% (w/v) bromophenol blue) and heated at 95°C for 4 minutes for SDS-PAGE analysis. Samples intended for COX analysis were heat at 40°C for 2 hours in the loading buffer to prevent COX protein aggregation.

2.5 Isolation of Bcl-2

Bcl-2 protein was found to bind agarose Protein A beads. Therefore, Bcl-2 was isolated from the protein lysate, by incubating two mg of heart protein with 50 μ L of agarose Protein A beads overnight at 4°C. The supernatant was removed and the beads with its bound protein (including Bcl-2) were resuspended in 250 μ L of loading buffer and heated as above to release the protein from the bead and obtain the protein in its primary structure.

2.6 Protein Analysis

50 μ g of protein heart lysate, 50 μ L of isolated Bcl-2, or 7 μ g of cardiac myocyte lysate (see below) was loaded on a 15% SDS-PAGE gel. Samples were electrophoresed at 200V for 1 hour. Proteins within the gel were then transferred to nitrocellulose using a wet transfer. Transfer buffer consisted of 192 mM glycine, 25 mM Tris, and 20% methanol. Membranes were then washed, dried, and kept at room temperature until needed. Upon probing, membranes were rehydrated in distilled H₂O for 5 minutes. Membranes were blocked with PBS pH 7.5 (TBS for Bcl-2) + 5% dry milk powder at room temperature with shaking for 1 hour. Primary antibody was then added at the determined concentration prepared in blocking solution and added for 1 hour. A rabbit anti-rat antibody was used for Bax (Oncogene, Cambridge MA) and caspase 3 (UBI Lake Placid NY) at 5 μ g/mL and 1/2000 dilution. For Bcl-2 and cytochrome C a monoclonal mouse anti-rat antibody was used at 1 μ g/mL (Transduction Laboratories, Lexington KY) and at 0.5 μ g/mL (Pharmingen, Mississauga Canada) respectively. Cytochrome oxidase subunit I (COX) involved an overnight incubation at 4°C with an antibody concentration

of 0.5 µg/mL (Molecular Probes, OR). Next, the membrane was washed with PBS + 0.1% Tween-20 for three 5 minute washes and one 15 minute wash. Secondary antibody was then added. This was either HRP-goat anti rabbit IgG (0.67 µg/mL, UBI) or biotinylated horse anti-mouse IgG, rat absorbed (2 µg/mL, Vector Laboratories, CA). Incubation of the secondary antibody was 30 minutes (rabbit) or 60 minutes (horse). The membrane was then washed as above. Membranes probed with horse anti-mouse were incubated with 0.2 µg/mL strepavidin-HRP for 30 minutes at room temperature. Blots were developed using ECL (Amersham, England) following manufacturer's instructions. Membranes were exposed to Hyperfilm™ ECL™ film (Amersham, England) and developed. Reprobed blots were stripped to remove bound antibody according to manufacture's instructions (Amersham). Detection of GAPDH was performed using a mouse monoclonal antibody (RDI, USA) at 0.01 µg/mL for 60 minutes at room temperature followed by the above detection system for a mouse primary. Actin was detected using the IgM clone 5C5 (Sigma) at 1/4000 dilution for 60 minutes at room temperature. A biotinylated anti-mouse IgM secondary (Vector Laboratories) at 2 µg/mL was used followed by strepavidin/HRP and ECL.

2.7 Caspase 3 Activity Assay

Caspase 3 activity was evaluated by measuring relative DEVDase cleavage activity. This assay also detects caspase 7 activity. Total-heart cell lysates (20 µL) were incubated with caspase-specific fluorescent substrate as described ⁷². Briefly, lysates were incubated with lysis buffer, without the protease inhibitors, containing 100 µM of the caspase substrate Ac-DEVD-AMC (Calbiochem, Cambridge, MA). The reaction mixture was

incubated at 37°C for 2 hours and fluorescence was measured using an excitation at 380 nm and an emission wavelength of 460 nm with a CytoFluor™ 2350 fluorescent measuring system (Perseptive Biosystems, Burlington, Ont). Background fluorescence was determined using an equal volume of the protein lysis buffer mixed with the above peptide.

2.8 TUNEL Staining

TUNEL was carried out using TdT-FragEL™ DNA Fragmentation Detection Kit (Oncogene, Cambridge MA). Control cells consisted of the positive and negative controls provided with the kit. An additional positive and negative control was heart tissue treated with 0.1 mg/mL DNase and heart tissue incubated without Tdt respectively. TUNEL staining was performed according to manufacture instructions. The degree of apoptosis was determined by a single blinded observer.

2.9 Isolation of Cardiac Myocytes

In separate experiments we measured fractional shortening of cardiac myocytes isolated from rats at multiple time points following LPS or PBS injection. Myocytes isolated from healthy, non-injected rats were used for the *in vitro* studies. Myocytes were isolated by collagenase digestion as previously described²⁴. Briefly, the heart was removed and washed twice in ice-cold MEM (minimal essential medium, Gibco BRL, Grand Island, NY). Within two minutes, the heart was hung by its aorta on a modified Langendorff apparatus. The heart then was perfused with 37°C oxygenated MEM to remove the remaining blood from the coronary circulation followed by perfusion with new re-

circulating MEM supplemented with 25 μ M calcium and 1 mg/mL of 230 U/g collagenase (type 2, Worthington Biochemical, Freehold, NJ). 10 to 15 minutes into the digestion the calcium concentration of the perfusate was increased stepwise to 50 μ M, followed by a further increase to 100 μ M 5 minutes later. Hearts were digested within 25-35 minutes as indicated by a "soft" heart. The ventricles from the soft heart were removed and gently teased apart. The teased tissue was then returned to the 37°C oxygenated MEM for a further 3 minutes. To separate individual myocytes from any undigested tissue the cell suspension was filtered through a 210 μ m nylon mesh. The filtrate was then centrifuged at 500 rpm for 4 minutes followed by re-suspension of the cells in MEM containing 200 μ M calcium. Removal of non-myocytes was achieved by gravity separation (myocytes pellet first due to their large size). The collected myocyte pellet, consisting of >99% cardiac myocytes, was re-suspended in MEM + 500 μ M calcium. Myocytes collected for the *in vitro* study were subject to two more gravity separation (MEM + 500 μ M calcium, MEM + 1000 μ M calcium) to remove most of the dead cells from the population. Myocytes for the *in vitro* study were resuspended in M199 (Gibco BRL, Canada) + 1% BSA. Cell concentration and % viable cells was counted using a hemocytometer.

2.10 *In Vitro* Challenge of Isolated Cardiac Myocytes

Myocytes in M199 + 1% BSA were plated in 24 well laminin coated plates at a density of 20 000 cells/well. Cells were re-fed at 90 minutes with M199 + 1% BSA and allowed to rest overnight. Sixteen to 18 hours after initial plating the myocytes were challenged with one or more agents diluted in M199 + 1% BSA. N in these experiments referred to

the number of separate wells in which the agent was tested. TNF α was tested at 5-200 ng/mL, IL-1 β at 5-10 ng/mL, combinations of TNF α and IL-1 β , staurosporine at 1-2 μ M, sphingosine at 1 μ M and 10 μ M, and camptothecin (Sigma) at 10-100 μ M. All challenges were carried out for 24 hours at 37°C and 5% CO₂. Fifteen minutes prior to the 24 hour time point, cells were trypsinized with 0.07% trypsin (30 μ L of 2.5% was added to the 1 mL of existing media) and returned to the incubator. Total cell population including those that were initially bound and those unbound were collected. Cells were then divided into one or more groups for analysis including fractional shortening, morphology, and TUNEL. Cells designated for TUNEL analysis were fixed in 4% formaldehyde for 15 minutes at room temperature followed by permeabilization with 80% ethanol. These cells were then cytopun at 1200 rpm for 4 minutes and stored at 4°C.

While cell isolation and culture was successful, as will be seen below, we were not successful in inducing apoptosis consistently. Thus, we were not successful in using the rat cardiac myocyte model to perform the pre-planned inhibition and mitochondria membrane potential studies.

2.11 Measurement of Cardiac Myocyte Contractile Function

Myocyte contractile function was measured as previously described²⁴. Briefly, myocytes were considered viable if they demonstrated a characteristic rod shape without cytoplasmic blebbing. This morphometric assessment of viability was confirmed in a subset of experiments with trypan blue exclusion. Specifically designed platinum electrodes were lowered into each well in the 96 well plate and the cardiac myocytes

were electrically stimulated (Grass S48 stimulator, W. Warwick, RI, 45 volts, 2.2 ms duration, 25 Ω resistance) while being recorded by videomicroscopy (Sony SLV-760HF). Still frames of systolic and diastolic myocytes were captured for computer analysis from the video recording. Fractional shortening was calculated as:

$$\% \text{ fractional shortening} = \frac{\text{diastolic length} - \text{systolic length}}{\text{diastolic length}}$$

2.12 Morphology Analysis of *In Vitro* Challenged Cardiac Myocytes

To determine whether the cardiac myocytes was viable, dead, or apoptotic, cells were stained with acridine orange and ethidium bromide. Cardiac myocytes were incubated on ice for 2 minutes in the presence of 10 $\mu\text{g/mL}$ of both acridine orange and ethidium bromide. Cells were then viewed using a fluorescent microscope with a FITC filter. Images were captured with the SPOT camera and stored digitally. Nuclei of viable cells will stain green, dead cells will stain red. Nuclei of apoptotic cells will still stain green but appear denser due to the chromatin clumping within the nuclei.

2.13 Cell Fractionation

Freshly isolated cardiac myocytes were resuspend in ice-cold cell fractionation buffer (20 mM HEPES pH 7.4, 10 mM KCl, 1 mM EDTA, 1 mM EGTA, 1.5 mM MgCl_2 , 250 mM sucrose, 1 mM PMSF, 1 U/mL aprotinin) followed by cell disruption with a dounce and 10 strokes with pestle B. Cells were kept at 4°C or on ice during the entire procedure. Cells were centrifuged at 800 X g for 10 minutes (nucleus), followed by centrifugation of

the supernatant at 10 000 X g for 15 minutes (mitochondria), and then again at 100 000 X g for 1 hour (supernatant = cytosol). Both the nuclear and mitochondria fractions were resuspend in ice-cold lysis buffer (20 mM Tris-HCl pH 8.0, 137 mM NaCl, 1% NP-40, 10% glycerol, 1mM PMSF, and 0.15 U/mL Aprotinin).

2.14 Statistical Analysis

We tested for differences over time compared to control using an analysis of variance.

When a significant difference was found ($p < 0.05$) we identified specific differences using Student t-tests corrected for multiple comparisons using a sequentially rejective Bonferonni test procedure.

CHAPTER 3: RESULTS

3.1 *In Vivo* Model

Bax mRNA levels increased following LPS injection relative to control (Figure 6A). Bax mRNA expression was maximum at 24 hours post LPS injection and was significantly greater than the control group ($p < 0.05$). Bax protein was expressed by the heart in all groups (Figure 6B). Bax protein expression decreased significantly from control baseline to 6 hours. At 12 hours, Bax protein expression continually increased above that at 6 hours resulting in a return to control values by 24 hours. Thus, regulation and expression of this early pro-apoptotic protein is altered in the heart by LPS injection.

LPS produced a different mRNA profile for Bcl-2 compared with Bax (Figure 7A). Heart Bcl-2 mRNA levels increased at 6 hours post LPS injection compared with controls ($p < 0.05$) and then returned to control levels by 24 hours. Bcl-2 protein showed a similar pattern to Bax (Figure 7B). Bcl-2 protein levels decreased substantially by 6 hours post LPS injection and then returned to baseline from the 6 hour time point to the 24 hour time point. Thus, regulation and expression of this early pro-survival pathway protein is altered in the heart by LPS injection.

While both Bax and Bcl-2 mRNA and protein changed in the heart following LPS injection, the pattern of expression is neither clearly pro-apoptotic nor pro-survival (Figure 8). Therefore, to determine if further pro-apoptotic signaling was triggered we first tested for cytochrome C release from the mitochondria. Cytochrome C was measured in the mitochondria and cytosol fractions of control and LPS treated rats at 6,

12, and 24 hours post injection. To ensure no contamination between the mitochondria and the cytosol fraction, the mitochondrial specific protein COX was measured (Figure 9). Only the mitochondrial fraction contained the COX protein, indicating no contamination. A pilot study of 2 rats per time point was tested to determine which time point cytochrome C was being released (Figure 9A). The pilot study indicated that cytochrome C was potentially being released at two potential time points, 6 hours and 24 hours. The 6 hour time point was chosen for further analysis based on this time point representing the maximum depressed cardiac function and the maximum change in Bax and Bcl-2 protein levels. Controlling for any protein loss and differences in protein loading on the gel, GAPDH and sarcomeric actin, two housekeeping proteins were also investigated. Cytochrome C levels were significantly lower in the mitochondrial fraction of the 6 hour LPS treated group compared with control ($p < 0.05$) (Figure 9B) indicating loss of mitochondria cytochrome C in the LPS group. The ratio of cytochrome C in the mitochondria compared to the cytosol was unchanged between control and the LPS group (Figure 9C).

To determine whether these changes in early apoptotic (Bax) and survival pathways (Bcl-2) were associated with activation of later steps leading to apoptosis, we investigated caspase 3 in the whole heart. Caspase 3 mRNA levels were unchanged throughout the experiment (Figure 10A), consistent with reports that caspase 3 is constitutively expressed^{73,74}. Caspase 3 protein analyzed by western blot identified the proform (32 KDa) but not the active fragment (17 KDa) at any time point (Figure 10B). Levels of the proform were unchanged during the 24 hour time period. Following LPS treatment

caspase 3 activity, as measured by cleavage of DEVD, continuously increased with maximum levels of 1000 fold greater ($p < 0.05$) than that produced by the control group at 24 hours (Figure 10C).

To determine whether this degree of caspase 3 activation led to end-stage apoptosis or whether survival pathways limited this progression we quantified TUNEL staining within the heart. Using TUNEL, no positive staining was seen in the viable control cells (provided with the kit) or in control heart tissue. Apoptotic cells within the LPS treated hearts were seen at all time points (Table 1, Figure 11). These apoptotic cells were seen as single cells and were present in both ventricles. A significant increase in TUNEL staining was observed at 24 hours post LPS injection compared with all other groups ($p < 0.05$) (Table 1). However, the fraction of apoptotic cells observed here was small.

Fractional shortening for cardiac myocytes isolated from control rats was $19.6\% \pm 0.6\%$. Fractional shortening decreased to $13.8\% \pm 0.5\%$ 6 hours after LPS injection ($p < 0.05$ compared to control), indicative of myocardial dysfunction. Myocardial function then improved towards the control value so that fractional shortening was $16.7\% \pm 0.67\%$ at 12 hours after LPS and did not increase further by 24 hours after LPS ($15.8\% \pm 0.7\%$) ($p < 0.05$ compared with control)(Figure 12).

3.2 *In Vitro* Model

Cardiac myocytes were challenged with a variety of agents for 24 hours (Figure 13, Table 2). $\text{TNF}\alpha$ showed a trend of increasing apoptosis with increasing dosage as determined by the TUNEL assay ($p=0.24$). Morphology analysis was inconclusive thereby not providing additional support (Figure 14). Both control and treated groups showed multinucleated myocytes. Myocytes were identified as dead if they contained an orange stained nuclei caused by the uptake of the ethidium bromide. Viable myocytes contained nuclei that were stained green. There also existed bright green nuclei that may have been the result of condensed chromatin, characteristic of apoptosis, but this additional characterization was not confirmed with the maximum magnification. Hence the identification of an apoptotic cell by this method at this magnification proved impossible. This same range of $\text{TNF}\alpha$ did not produce any cardiac depressant effect as measured by fractional shortening.

Challenge of cardiac myocytes with $\text{IL-1}\beta$, $\text{IL-1}\beta$ and $\text{TNF}\alpha$, sphingosine, staurosporine, Fas, or camptothecin did not result in a significant increase in apoptosis (Table 2).

Cardiac myocyte function as measured by fractional shortening was either inconclusive or unchanged by any of these agents. Within any population a certain percentage will have a small contraction. Thus, to properly determine the effect of these agents on cardiac function, fractional shortening of many more myocytes needs to be measured.

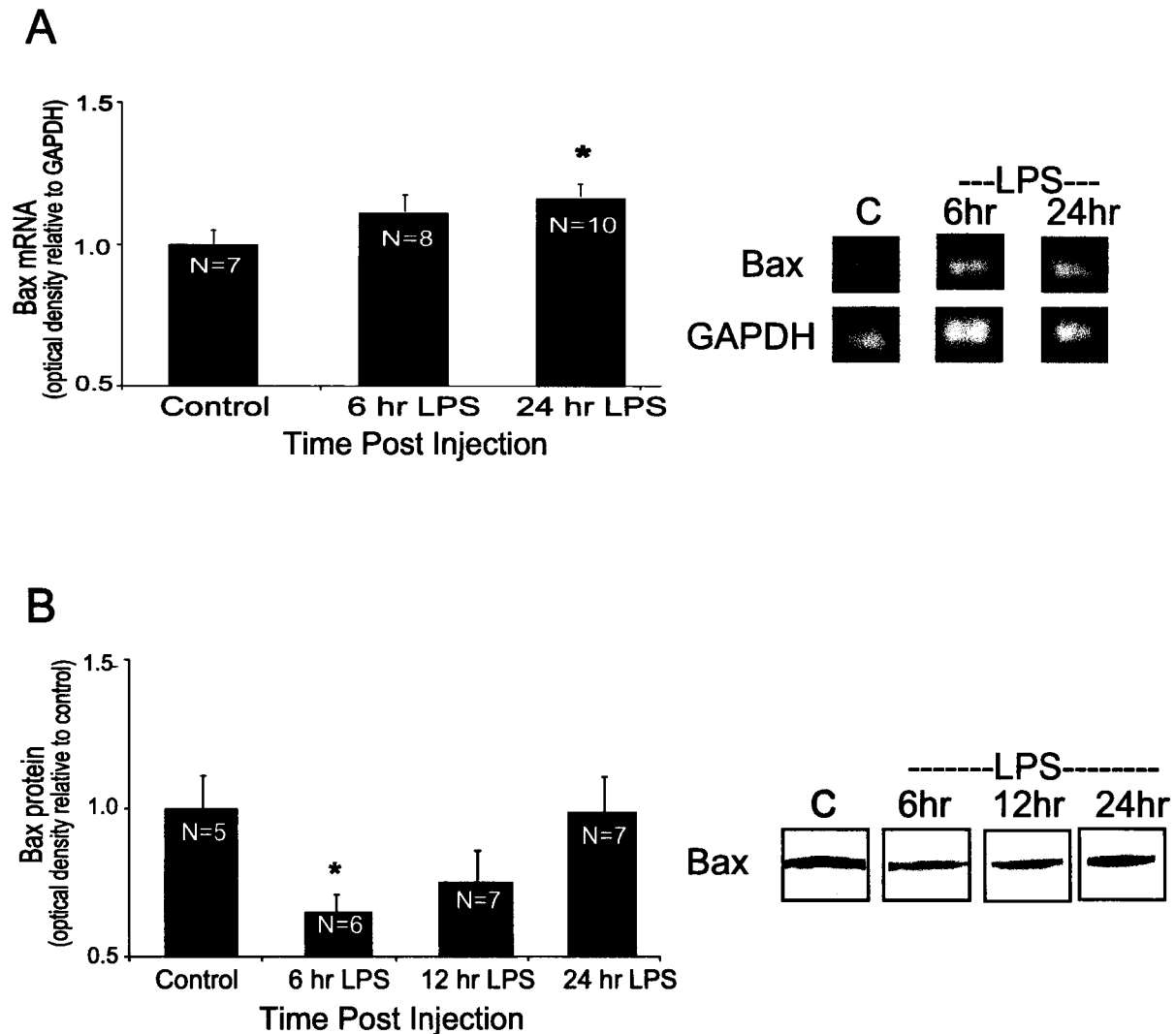


Figure 6. Effect of LPS on heart Bax mRNA and protein levels. A) Graphical representation of Bax RT-PCR results based on densitometry analysis relative to their respective GAPDH densitometry. Results are normalized to control samples. B) Graphical representation of Bax western blot based on densitometry analysis. Results are normalized to control. * $p < 0.05$ compared with control. Results are expressed as mean \pm SE.

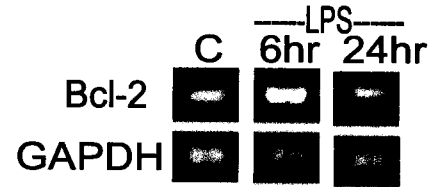
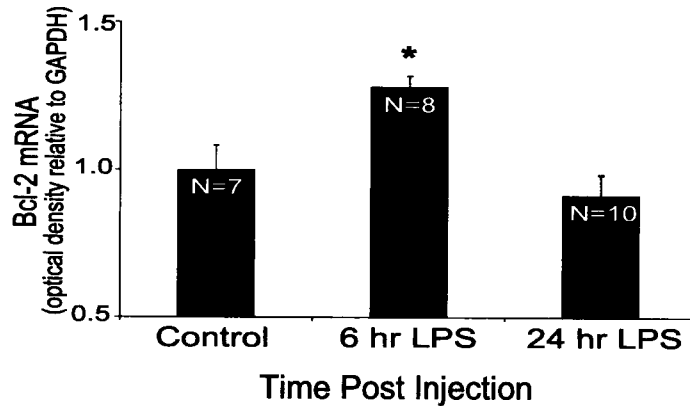
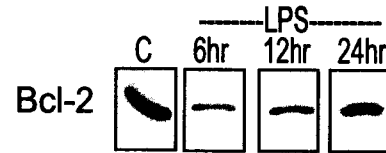
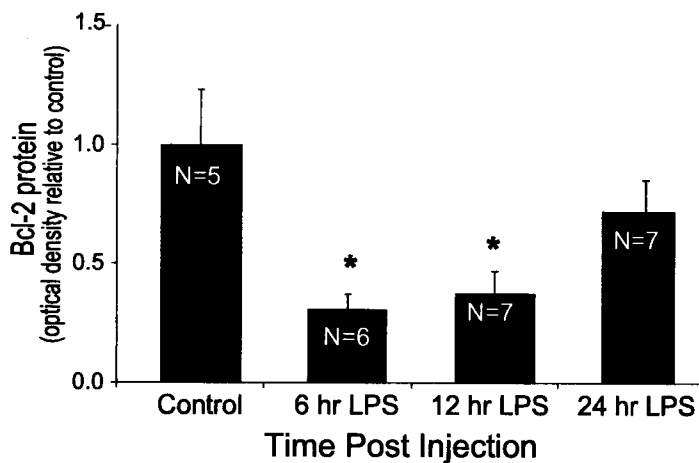
A**B**

Figure 7. Effect of LPS on heart Bcl-2 mRNA and protein levels. A) Graphical representation of Bcl-2 RT-PCR results based on densitometry analysis relative to their respective GAPDH densitometry. Results are normalized to control samples. B) Graphical representation of Bcl-2 western blot based on densitometry analysis. Results are normalized to control. * $p < 0.05$ compared with control. Results are expressed as mean \pm SE.

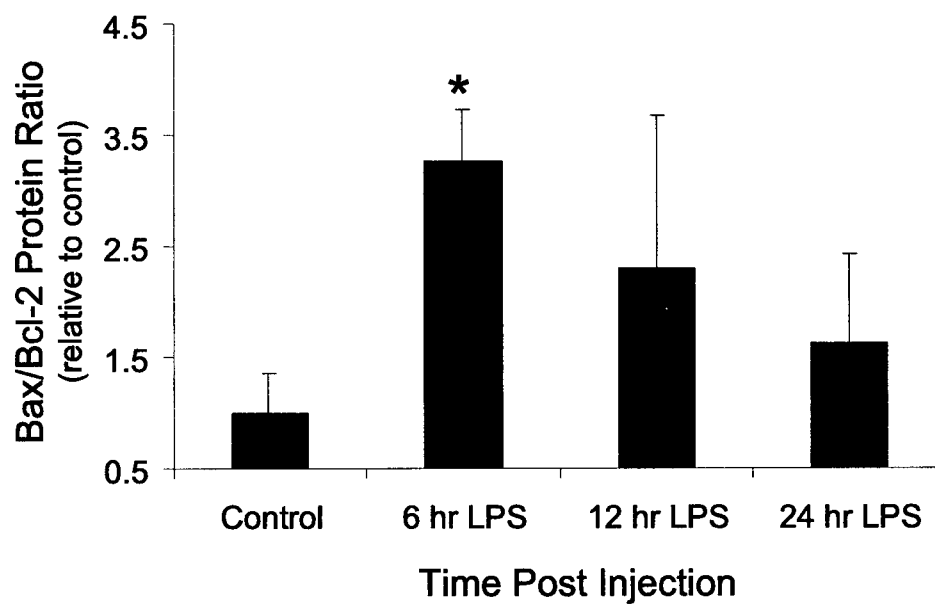


Figure 8. Effect of LPS on heart Bax/Bcl-2 protein ratio. Graphical representation of Bax western blot densitometry results compared with the corresponding Bcl-2 western blot densitometry results. Results are normalized to control. Results are expressed as median \pm SE.

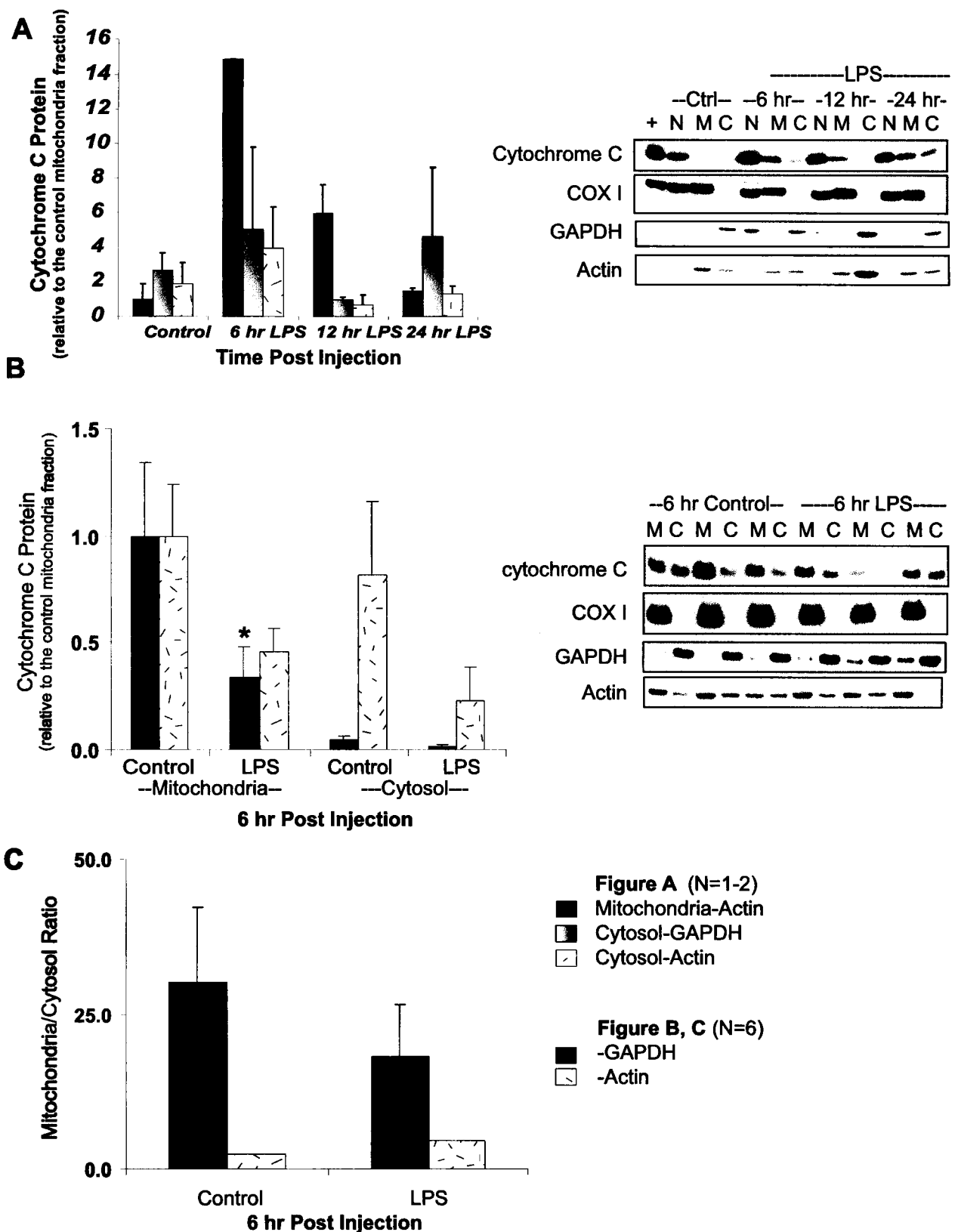


Figure 9. Effect of LPS on cardiac myocyte cytochrome C levels. A) Graphical representation of the mitochondria and cytosol fraction cytochrome C level relative to GAPDH or sarcomeric actin. Results are normalized to control and accounted for % non-viable cells. The accompany representative western blot includes analysis of the mitochondria specific COX I protein. Western blot labeling includes N denotes nuclear fraction, M denotes mitochondria fraction, and C denotes cytosol fraction. B) Same as in A) but 6 hours post LPS injection. C) Graphical representation of results in B) expressed as the ratio of cytochrome C in the mitochondria/cytosol. * $p < 0.05$ compared with control. Results are expressed as mean \pm SE.

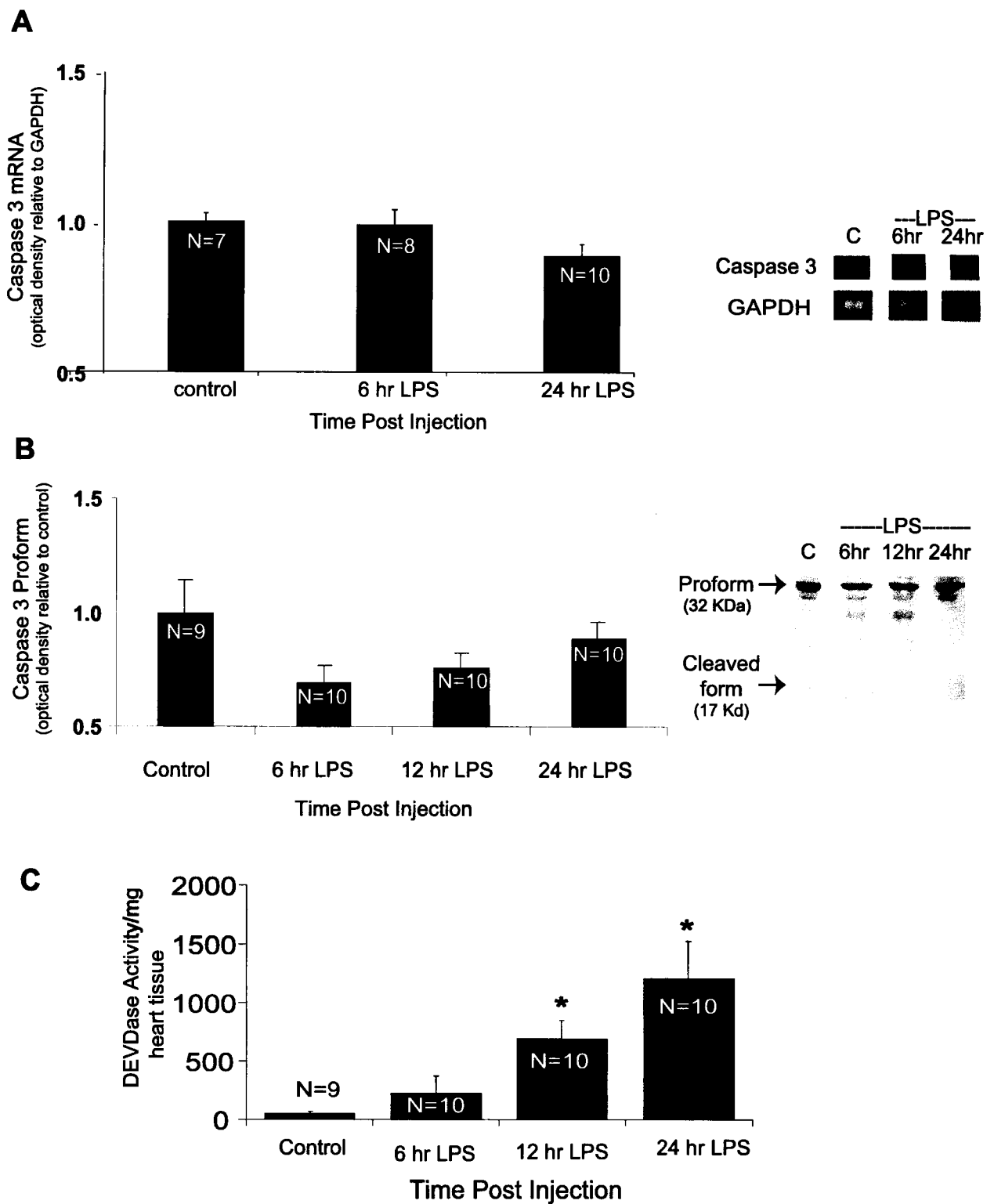


Figure 10. Effect of LPS on heart caspase 3. A) Graphical representation of RT-PCR results based on densitometry analysis relative to their respective GAPDH densitometry. Results are normalized to control samples. B) Graphical representation of pro-caspase 3 western blot based on densitometry analysis. Results are normalized to control. C) Graphical representation of fluorescent intensity as derived from DEVD cleavage. * $p < 0.05$ compared with control. Results are expressed as mean \pm SE.

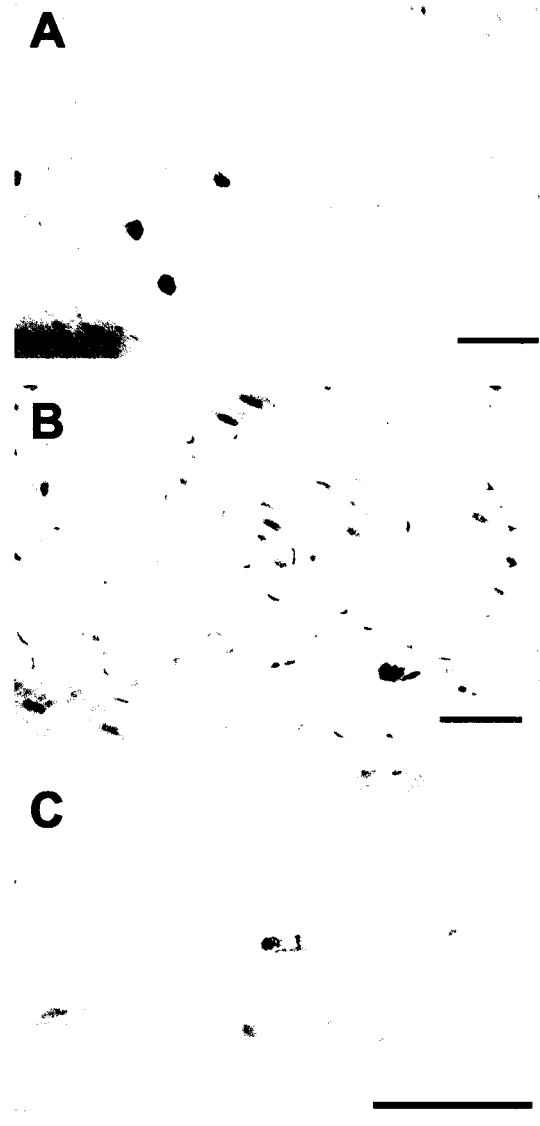


Figure 11: In situ labelling of heart DNA fragmentation. TUNEL labeled fragmented DNA brown. Tissue sections were counterstained with methylene blue producing a green nucleus. A) control, B) DNase treated (0.1 mg/mL), C) 24 hour LPS. Bar represents 50 μ m.

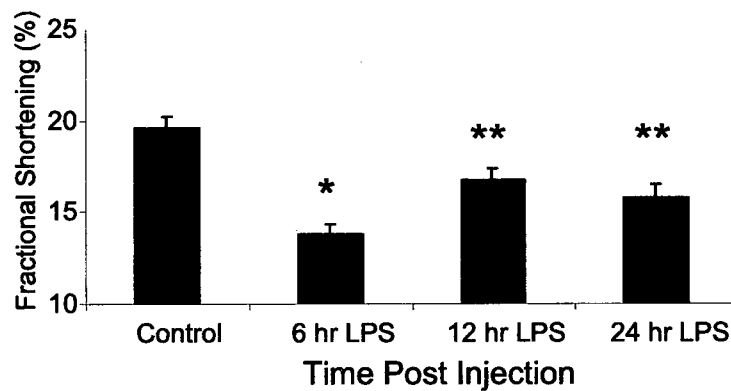


Figure 12. Effects of LPS on cardiac myocyte contractility. Graphical representation of % fractional shortening as derived from (diastolic - systolic length)/diastolic length. * <0.05 compared with control. ** $p<0.05$ compared with control and 6 hour LPS. N=30-35 myocytes/animal with 2 animal/group. Results are expressed as mean \pm SE.

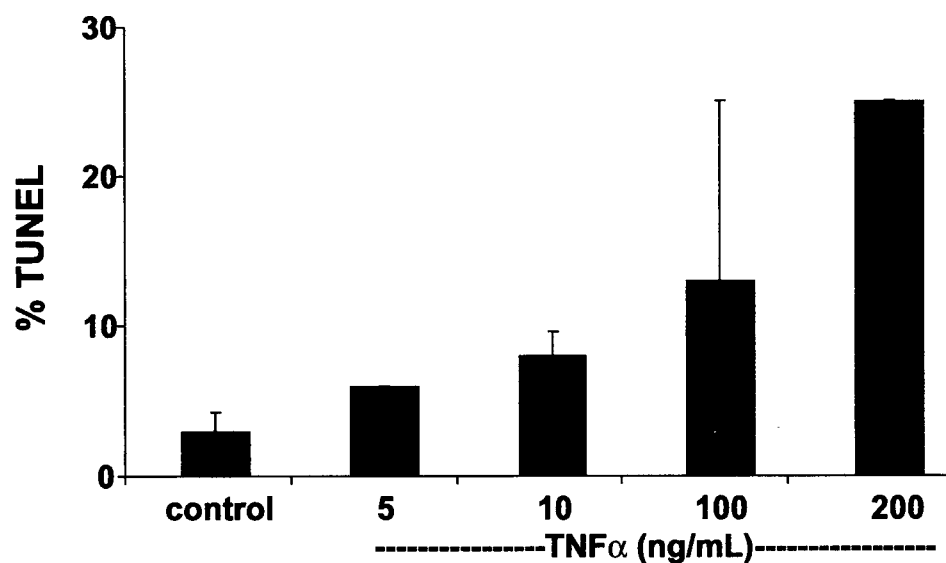
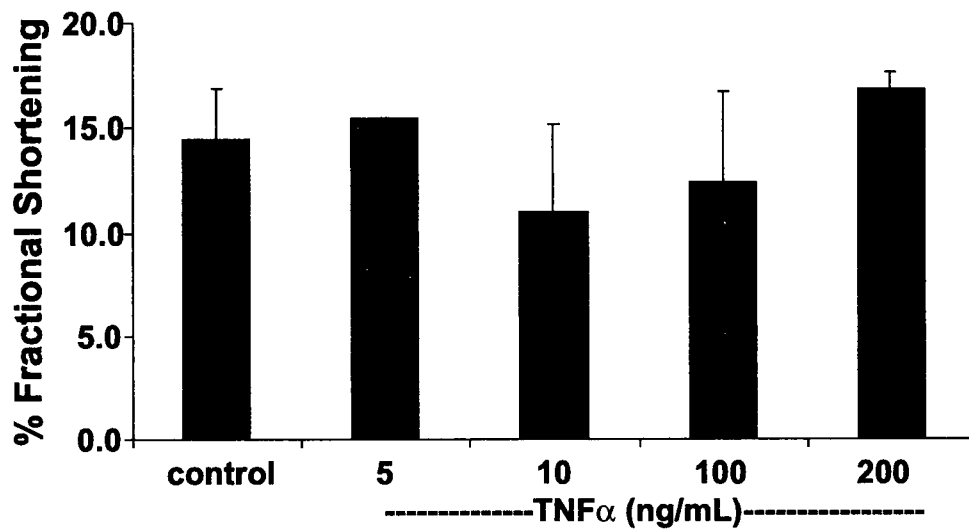


Figure 13. *In vitro* effect of TNF α on cultured cardiac myocytes. A) 24 hour TNF α influence on adult cardiac myocyte function as determined by % fractional shortening. B) 24 hour TNF α influence on adult cardiac myocyte apoptosis. N=2-3 where N implies the number of wells. Results expressed as mean \pm SE.

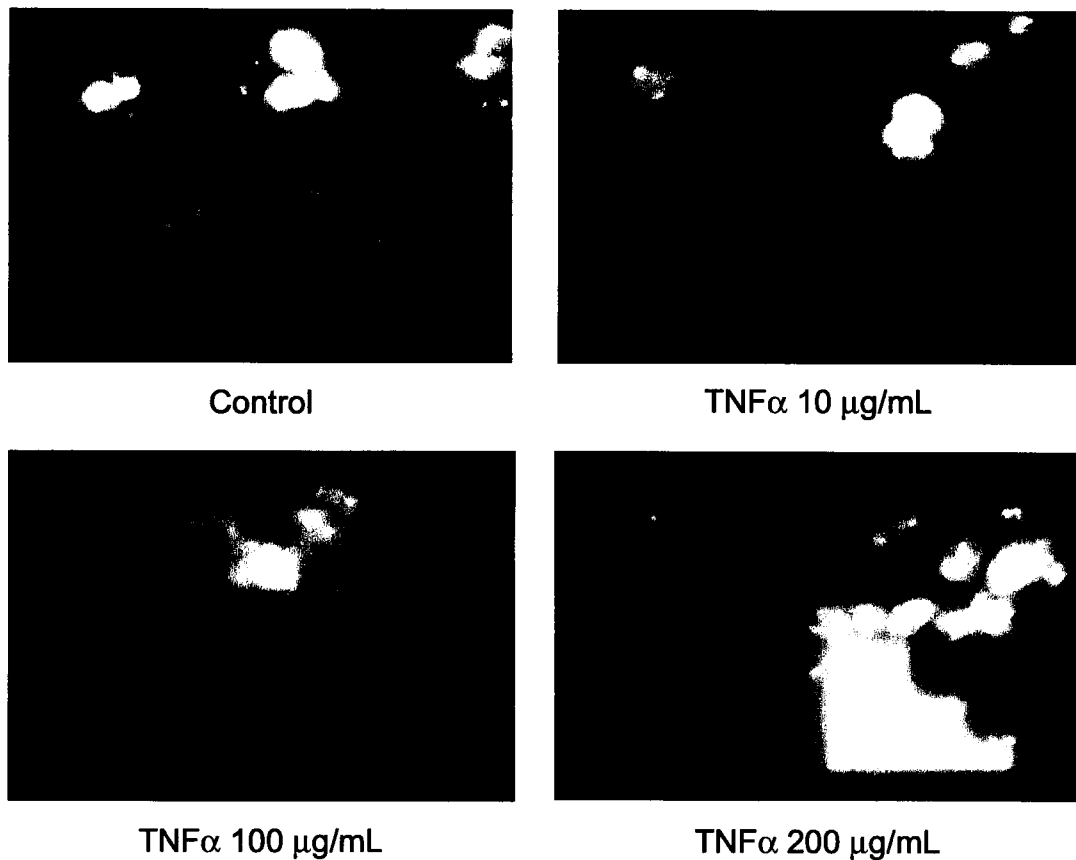


Figure 14. TNF α effect on the survival of adult cardiac myocytes after 24 hour exposure. Cardiac myocytes are stained with acridine orange and ethidium bromide. Viable cells stain green. Early-stage apoptotic cells stain green but with greater intensity than control cells and they present themselves with a smaller nuclei. Late-stage apoptotic and necrotic cells stain red. Magnification 400X.

| Time Post LPS Injection | Number of TUNEL positive cells per cross section of heart |
|-------------------------|---|
| ≤4 hr | 2.3 ± 1.0 |
| 8 hr | 2.7 ± 1.2 |
| 12 hr | 4.3 ± 3.8 |
| 24 hr | 10.3 ± 4.7* |

Table 1: TUNEL results of LPS treated hearts. Numbers represent mean ± SE. *
p<0.05.

| Treatment Group (24 hours) | % TUNEL | % Fractional Shortening |
|-------------------------------|-----------------|-------------------------|
| Control | 3 ± 1.2 (N=5) | 14.5 ± 2.4 (N=8) |
| IL-1β 5 ng/mL | 12 (N=1) | 6.3 (N=1) |
| IL-1β 10 ng/mL | 8.5 ± 2.5 (N=2) | 17.4 ± 1.8 (N=2) |
| TNFα /IL-1β 1/1 ng/mL | 3 (N=1) | 15.8 ± 3.5 (N=2) |
| TNFα /IL-1β 5/5ng/mL | 13 (N=1) | 21 (N=1) |
| TNFα /IL-1β 10/10 ng/mL | 4 (N=1) | 19.4 ± 6. 8 (N=3) |
| Sphingosine 1 μM | 16 (N=1) | - |
| Sphingosine 10 μM | 10 (N=1) | 12.0 ± 3.6 (N=2) |
| Staurosporine 1 μM | 4.3 ± 2.3 (N=3) | 21.2 (N=1) |
| Staurosporine 2 μM | 9.7 ± 3.8 (N=3) | 7.3 (N=1) |
| Fas 100 ng/mL | 0 (N=1) | 17.8 ± 1.2 (N=3) |
| Fas 200 ng/mL | 6 (N=1) | 17.5 ± 4.2 (N=5) |
| Camptothecin 10 μM | 3 ± 0 (N=2) | - |
| Camptothecin 100 μM | 3 ± 2 (N=2) | - |

Table 2. Effect of apoptosis inducing agents on adult cardiac myocytes during a 24 hour exposure. Numbers represent the percentage mean ± SE. N refers to the cardiac myocyte population in a given well (N=1 implies 1 well and 1 population).

CHAPTER 4: DISCUSSION

Myocardial dysfunction occurs during sepsis yet the mechanism is not completely understood. Myocardial apoptosis may be one contributing factor to this clinical observation. The purpose of this study is to focus on the possibility that apoptosis may occur in the heart during sepsis. By investigating both apoptotic and survival pathways I hope to convince you that these pathways are activated and their potential influence on myocardial dysfunction is an important area of research.

4.1 Summary of Main Findings

In this rat LPS model of sepsis we found evidence of activation of both apoptotic and survival pathways as early as 6 hours after LPS injection. By 24 hours we found evidence of activation of later apoptotic pathways and evidence of end-stage apoptosis of myocardial cells using TUNEL staining. Evidence of involvement of apoptotic pathways was associated with a partially reversible decrease in myocyte fractional shortening. The maximal decrease in fractional shortening was temporally associated more closely with mitochondria-related apoptotic pathways than with end-stage apoptosis. The absolute number of apoptotic cardiac myocytes is likely insufficient to account for myocardial depression of sepsis but it is conceivable that apoptotic and survival pathways, and particularly their relationship to mitochondrial function, may contribute to myocardial dysfunction of sepsis and acute inflammation.

To further investigate the association between apoptosis and myocardial dysfunction an *in vitro* model was attempted. Cultured cardiac myocytes proved resistant to a variety of

apoptosis-inducing agents. One possible exception was TNF α , which caused a trend to increased cardiac myocyte apoptosis. However, this concentration of TNF α had minimal adverse effects on myocardial function. An *in vitro* model of cardiac myocyte apoptosis requires further work. Lack of an *in vitro* model does not contradict the findings of the septic *in vivo* model but makes identifying mechanistic pathways more difficult.

4.2 Bax versus Bcl-2 in the LPS Rat Model

Myocardial dysfunction present during sepsis is known to involve the mitochondria⁷⁵⁻⁷⁷. Interestingly, fate of a cell can be highly influenced by the mitochondria; specifically by the Bcl-2 family of proteins³². Two members, Bax and Bcl-2 promote apoptosis or survival respectively. Their involvement in cell fate has even been shown within the heart⁷⁸. Hence they were chosen for investigation in the septic heart both at the mRNA and the protein level.

In order to show that LPS affects the pro-apoptotic Bax pathway and the pro-survival Bcl-2 pathway, their respective mRNA levels were determined. We found that LPS affects both Bax and Bcl-2 mRNA expression. mRNA expression can be increased by increasing transcription of the gene or by increasing the stability of the mRNA. The increase in Bcl-2 mRNA at 6 hours post LPS injection likely contributed to the corresponding rise in protein seen at 12 and 24 hours. Bax mRNA levels did not increase significantly until 24 hours post LPS injection. Thus the rise in Bax protein from 6 to 24 hours was not the result of increased Bax transcription but the result of increased translation. The effect of the small but significant increase in Bax mRNA at 24 hours

was not investigated but suggests that apoptotic pathways are still influenced by downstream mediators of LPS. It was not surprising to find Bax mRNA levels effected by LPS since the cytokines IL-1 β and IFN- γ have been shown to influence these levels in the neonatal myocyte ⁷⁹. However, the degree of influence on Bax mRNA was 10%-20% in this rat model compared to the 10 fold increase seen in the IL-1 β and IFN- γ challenged neonatal myocytes. Two contributing factors for these differences include *in vivo* versus *in vitro* and adult versus neonatal. *In vivo* conditions present many complex interactions that are not present in a simple single cell type cell culture and, as such may counteract the strong pro-apoptotic Bax signal. Adult versus neonatal will also likely play a role since their sensitivity to apoptosis is different ⁶⁵. Bcl-2 mRNA levels can also be dynamic as noted during postnatal heart development where levels drop dramatically at day 1 post birth followed by a rise days 5 to 21 post birth ⁶⁰. *In vitro* studies ^{80,81} indicate that both Bax ⁷⁹ and Bcl-2 ⁸² mRNA levels can change in the adult myocyte. Thus changes in Bax and Bcl-2 mRNA presented in this rat model of sepsis are in agreement with other studies indicating that their mRNA levels can be regulated.

In our model of sepsis we observed that, at six hours after LPS injection, Bax and Bcl-2 protein expression declined and then gradually returned to control levels by 24 hours. LPS directly or indirectly appears to be capable of regulating Bax and Bcl-2 protein levels independently of their mRNA. For instance, the half-life of Bax and Bcl-2 protein decreases in response to inflammatory stimuli ⁵⁴. More specifically caspases and other proteins involved in apoptosis can cleave and inactivate or down regulate the Bcl-2

family of proteins ^{44,83}. Thus, the early decrease in Bax and Bcl-2 that we observed might be explained by destruction or shortened half-life of these proteins.

In vivo studies including analysis of the heart's Bax and Bcl-2 protein indicate that a wide variety of responses are possible. Olivetti and colleagues ⁵⁹ studied patients who died of chronic heart failure. An increased number of apoptotic myocytes was accompanied by a doubling of Bcl-2 protein in these cells with no change in Bax protein as determined by immunohistochemistry ⁵⁹. These results were taken to imply that the heart was attempting to avoid end-stage apoptosis. A study investigating myocardial infarction in young (6-8 months) Harlan Sprague Dawley rats demonstrated a decrease in Bax protein with a corresponding increase in Bcl-2 protein levels ⁷⁸. This ratio favoring Bcl-2 was high even at the time of maximum DNA fragmentation in the cardiac myocyte. In contrast, other studies looking at the progression of left ventricular hypertrophy (LVH) to left ventricular dysfunction (LVD) showed an increase in Bax and a decrease in Bcl-2 for the whole heart. The Bax/Bcl-2 ratio favored Bax and more prominently with progression to LVD ³⁷. As well, both Bax and Bcl-2 protein can increase in the heart, as observed during coronary occlusion ⁸⁴. All of the above studies showed a different Bax/Bcl-2 response from that seen in this septic rat model.

In our study, we also saw limited but significant increase in end-stage apoptosis. At the time of maximum TUNEL positive cells both Bax and Bcl-2 levels had returned to baseline values. Thus the increase in Bax/Bcl-2 ratio at 6-12 hours post LPS injection was disassociated with DNA fragmentation. At no time through out the experiment were

changes from baseline Bcl-2 protein levels higher than changes in Bax levels or control values. As well Bax levels did not remain constant nor did they increase above control levels. These differences indicate that LPS has a different effect on the Bcl-2 family within the heart.

Our analysis of Bax and Bcl-2 in the whole heart does not indicate which cell type(s) are affected. A variety of cell types present within the heart express or can be induced to express Bax and Bcl-2. In health, smooth muscle cells, neutrophils, macrophages, and myocytes have detectable levels of the Bax protein ^{38,59,85,86}. Bcl-2, is however, only detectable in smooth muscle cells and macrophages in healthy individuals ^{38,86}.

Neutrophils, when challenged *in vitro* with LPS, show no change in Bax protein levels and no detectable levels of Bcl-2 ⁸⁵. Hence, the fluctuation in Bax and Bcl-2 protein levels are unlikely to be contributed by the neutrophil. Macrophages undergo accelerated rates of apoptosis but the involvement of Bax and Bcl-2 are unknown ⁵¹. Thus, potential contributing sources to the decrease in Bax protein levels present at 6 hours post LPS injection are smooth muscle cells, cardiac myocytes, and possibly macrophages. As indicated above, immunohistochemistry studies of *in vivo* myocytes indicate that Bax and Bcl-2 protein can decrease or increase within cardiac myocytes ^{59,78,84}. Thus it is feasible that the changes in Bax and the increase in Bcl-2 protein include those present in the cardiac myocyte. The initial decrease in Bcl-2; however, is not likely affected by cardiac myocytes since, in health, they have undetectable levels.

LPS affects the heart by activating both apoptotic and survival pathways as shown by the changes in Bax and Bcl-2 mRNA and protein. These changes are likely at least partially attributable to changes occurring within the cardiac myocyte. The effect these changes have on the heart is unclear because neither the apoptotic Bax pathway nor the survival Bcl-2 pathway clearly dominated. Further supporting evidence for the uncertainty of these pathways on cell fate, is the lack of increased end-stage apoptosis (see TUNEL discussion) at the time of maximum ratio (6 hours). This correlation would be expected if the cells are pro-apoptotic in nature because the *in vivo* apoptotic process would be initiated at different times in different cells and therefore a rise in TUNEL positive cells at 6 hours and perhaps at 12 hours was expected. The potential favor of the apoptotic Bax pathway at 6 hours may not have reached the apoptosis-inducing threshold or it may be counter-acted by other pro-survival proteins such as Mcl-1 or Bcl-xl. The presence of these other proteins from the Bcl-2 family were not investigated due to the lack of available rat antibodies. The heart responded and adapted to the LPS insult as shown by the activation of apoptotic and survival pathways. The effect of this response and adaptation is not accompanied by cell death but perhaps by heart dysfunction.

4.3 Are Mitochondria Involved in LPS induced Cardiac Apoptosis?

In this model of acute sepsis both Bax and Bcl-2 protein levels declined and then rebounded so that the pattern of expression was neither clearly pro-apoptotic nor pro-survival. On the one hand, the decrease in Bcl-2 by western blot was greater than the decrease in Bax, potentially favoring apoptosis. To address this issue we determined the net effect of Bax promoting and Bcl-2 inhibiting mitochondrial cytochrome C release

40,43-45. Mitochondria have been shown to be frequently involved in apoptosis via the release of cytochrome C^{43,45}. As well, TNF α and nitric oxide have been shown to involve the mitochondria when inducing apoptosis⁸⁷⁻⁹⁰. A pilot study was done to investigate cytochrome C levels at all time points. The results from this cytochrome C pilot study (maximum difference at 6) and the time of maximal change in Bax and Bcl-2 protein lead us to investigate cytochrome C release at 6 hours post LPS. We also chose to only investigate cytochrome C in cardiac myocytes because these cells are affected by myocardial dysfunction.

Cytochrome C levels showed a trend towards lower levels in the mitochondrial fraction of the 6 hour LPS treated group compared with the 6 hour PBS control group by approximately one-half ($p=0.06$ for actin; $p=0.09$ for GAPDH). However, cytosol levels of Cytochrome C, when normalized to GAPDH, also showed a trend towards lower amounts in the LPS group compared with controls ($p=0.17$). Whereas, when cytosol cytochrome C levels are normalized to sarcomeric actin no difference was detected ($p=0.55$). The discrepancy between these two housekeeping proteins may reside in GAPDH being a cytosol protein and actin being a structural protein. The differences between these two types of proteins may be important due to the experimental isolation procedure. Individual myocytes were isolated by enzymatic digestion. Myocytes damaged from this isolation method or by the *in vivo* response to the LPS, may have lost internal proteins during the isolation procedure. GAPDH may control for loss of these proteins better than the structurally protein, actin. Thus the cytosol cytochrome C level is more accurately reflected by the those values normalized to GAPDH, although the

difference between groups is still not significant ($p=0.17$). The ratio of mitochondria to cytosol cytochrome C levels when normalized to either GAPDH or actin showed no statistical difference ($p=0.46$ GAPDH; $p=0.41$ for actin). To ensure that the cytochrome C detected in the cytosol fraction was not contaminated with cytochrome C from the mitochondria the mitochondria specific COX-I subunit was also detected. COX-I was only detected in the mitochondria fraction confirming no contamination of the cytosol. There was also no detectable COX I protein differences between the LPS and the control group. The myocyte isolation procedure results in a 40% to 60% death rate. This high death rate explains why all fractions from both groups contain cytochrome C. We can conclude from these results that only mitochondria levels of cytochrome C show any potential difference between the LPS and the control group.

The decrease in mitochondrial cytochrome C level, the potential decrease in cytosol cytochrome C level, and no change in mitochondria/cytosol ratio can be the result of many possible scenarios. The 6 hour LPS group appears to have less cytochrome C overall. The mitochondria fraction from the 6 hour LPS group has less cytochrome C and therefore less cytochrome C is able to escape to the cytosol. Loss of cytochrome C due to the isolation procedure has been accounted for by normalizing the results to the housekeeping proteins. Cytochrome C is capable of binding many proteins including its anchor protein cardiolipin ⁹¹, Bcl-2 ⁴³, Bax ⁹², and nitric oxide ⁹². These interactions were dissociated when the sample was heated in the SDS sample buffer as confirmed by molecular weight and; therefore, should not have interfered with antibody detection. Mitochondria cytochrome C levels drop in *Trypanosoma cruzi* infected rats ⁹³, and in

ischaemic tissue ⁹⁴. In both of these articles there is no mention of analysis of cytochrome C in the cytosol. As well, cytochrome C will decrease in the mitochondria during apoptosis ⁹⁵. Cytochrome C release from the cardiac myocyte *in vivo* has not been clearly shown. Idiopathic dilated cardiomyopathy and ischemic cardiomyopathy have shown cytochrome C release from the mitochondria but without identification of cell type ⁹⁵. *In vitro* studies indicate that cytochrome C release is possible from cardiac myocytes ⁹⁶. Hydrogen peroxide challenged neonatal myocytes showed cytochrome C release but this was not induced using other free oxygen radicals ⁹⁶. Reasons for the loss of cytochrome C from mitochondria in this septic model are unknown. Possible scenarios include a depressed transcription or translation of the gene, degradation within the mitochondria, or degradation within the cytosol after released from the mitochondria. Transcription of cytochrome C in the rat heart may be oxygen dependent as it is in yeast ⁹⁷. Sepsis is accompanied by hypoxia but not within the heart ^{98,99}. As well, other rat models similar to ours have not reported cardiac hypoxic conditions ¹⁰⁰. Thus decrease in cytochrome C transcription is unlikely. The decrease in mitochondrial cytochrome C level may be part of a negative feedback mechanism. In septic baboons the mitochondrial activities of complex I and complex II are reduced ⁷⁵ which may negatively influence cytochrome C levels. The decrease in mitochondria cytochrome C without a rise in cytosol cytochrome C may still indicate the presence of apoptosis. The connection to apoptosis and the fact that both Bax and Bcl-2 can influence mitochondria cytochrome C levels by interacting with it directly or indirectly indicates that the changes in Bax and Bcl-2 that we observed potentially contribute to some of the mitochondrial cytochrome C loss. The Bax/Bcl-2 ratios at 6 hours post LPS favors Bax and therefore

potentially cytochrome C releases. This time point was associated with a loss of cytochrome C from the mitochondria. The explanation for the lack of rise in the cytosol fraction is unknown. Bobba and colleagues have reported that cytochrome C will degrade in the cytosol by a caspase mediated event ¹⁰¹. Cytochrome C degradation from the cytosol was blocked with z-VAD-fmk, a broad spectrum caspase inhibitor ¹⁰¹. At this 6 hour time point we did not observe an increase in caspase 3 activity, but the activity of other caspases are unknown. Therefore, it is possible that this lack of cytochrome C recruitment in the cytosol may not rule out activation of further apoptotic pathways.

The effect of this decreased cytochrome C may decrease ATP production, increase oxidants, or induce apoptosis. Cytochrome C shuttles electrons between complex III and IV of the mitochondrial respiratory chain to generate ATP. A break in this system by the loss of cytochrome C may reduce ATP production levels. Supporting evidence for a disruption in electron transport chain in the heart during sepsis, comes from MTS assays ^{76,77} and by the identified disruption of complex I and II of the mitochondria respiratory chain ⁷⁵. Others however, have reported no loss in ATP during sepsis ¹⁰². Cytochrome C is a key regulator of limiting the amount of superoxide production by the mitochondria ¹⁰³. Thus a decrease in cytochrome C as seen in this LPS rat model may lead to a rise in superoxide which in turn will negatively influence cardiac function and lead to potential rise in apoptosis ^{92,104}. Indeed, in septic and LPS rat models an increase in superoxide has been reported ¹⁰⁵.

We have found that cardiac myocytes contain lower levels of cytochrome C within their mitochondria as the result of LPS exposure. This loss of mitochondria cytochrome C was not accompanied by a concurrent rise in the cytosol. The effect of this depressed mitochondria cytochrome C may contribute to the decrease in cardiac function as this 6 hour time point (see function paragraph). The reason for this decrease in mitochondrial cytochrome C is unknown but may be influenced by the change in Bax and Bcl-2 protein levels.

4.4 A Minimum of One Apoptotic Pathway was Activated in the LPS-Treated Heart

Caspases are executioners of apoptosis³². Caspase 3 was chosen for investigation due to its unique role as being the central executioner of apoptosis, for it represents a junction point for many apoptotic pathways (Figure 2). Activation of caspase 3 implies that a minimum of one upstream apoptotic pathway was activated. This includes activation by other caspases and by cytochrome C and AIF release from the mitochondria. Caspase 3 exists in an inert form in the cytosol until cleaved by other caspases. To confirm caspase 3 is constitutively expressed in this LPS rat model, mRNA levels were investigated. Active caspase 3 was investigated by looking for its cleaved active fragment and by the enzymatic activity of this cleaved fragment.

In this LPS rat model, caspase 3 mRNA levels were constant indicative of the gene being constitutively expressed. Presence of the active caspase 3 protein can be determined in two ways using a western blot: 1) loss of the proform protein, and 2) presence of the active form. The antibody used in this study detects both the inactive and active form of

caspase 3. Western blot analysis indicated no detectable decrease in the proform and no presence of the active form. It can be difficult to detect the active form due to its degradation. The heart's heterogeneity may also make it difficult to detect the active form if few cells are undergoing apoptosis. Caspase 3 activity as measured by its ability to specifically cleave the amino acid sequence DEVD, indicated that caspase 3 was activated in the heart. Caspase 3 activity increased with time post LPS to levels of 1000 fold above control values. Caspase 3 activity assay proved to be more sensitive than the western blot analysis.

Caspase 3 activation is a key finding and confirms that at least one apoptotic pathway has been activated. The correlation between caspase 3 activity and end-stage apoptosis has been shown by others ^{58,81,106}. In this study, increasing caspase 3 activity correlated with an increase in apoptosis. The exact amount of active caspase 3 needed to induce end-stage apoptosis is unknown. Previous reports of caspase 3 activity in the heart have only been shown using an antibody to the active form of the caspase ¹⁰⁶. This is the first reported case of increased caspase 3 activity in the heart in a model of sepsis, as measured by its ability to cleave the amino acid sequence DEVD. The source of this caspase 3 activity in the heart is unknown because total heart lysate was tested. In healthy hearts myocytes, fibroblasts, and smooth muscle cells have detectable levels of the caspase 3 inactive proform by immunohistochemistry ⁷³. Thus cardiac myocytes could be contributing to the increased level of caspase 3 activity.

Cardiac myocytes have the ability to activate their own caspases including caspase 3^{96,106-108}. Caspase 3 can be activated within the cardiac myocyte by ischemia/reperfusion¹⁰⁶, and *in vitro* with staurosporine, doxorubicin, or hydrogen peroxide^{80,96,108}. Although caspase 3 activation is possible in the cardiac myocyte, the extent to which cardiac myocytes contribute to the observed whole-heart increase in caspase 3 activity is unknown. Black's study on ischemia/reperfusion only found cardiac myocytes to be TUNEL and/or caspase 3 positive and not the infiltrating neutrophils or macrophages¹⁰⁶. During sepsis macrophage apoptosis is accelerated whereas neutrophil apoptosis is delayed^{51,56,57}. Whether caspase 3 plays a role in macrophage and neutrophil apoptosis in this LPS heart is unknown. Smooth muscle cells responding to TNF α also increase caspase 3 activity¹⁰⁹. Stimulation of fibroblast in culture with IL-1 β , IFN- γ , TNF α or nitric oxide for 5 days did not induce apoptosis¹¹⁰. However, these same cytokines were able to induce apoptosis in smooth muscle cells¹¹¹. Glomerular endothelial cells have also shown to activate caspase 3 after exposure to LPS¹¹².

This is the first report of caspase 3 activity as measured by DEVDase in the *in vivo* heart. Caspase 3 levels increase at 12 hours post LPS followed by a further increase at 24 hours post LPS. Cardiac myocytes likely contribute to the levels detected in the whole heart lysate. Other cells potentially contributing to caspase 3 activity include leukocytes, smooth muscle and endothelial cells. The detection of caspase 3 activity confirms that apoptotic pathway(s) have been activated in the heart. Caspase 3 activity is associated with a small degree of end-stage apoptosis in myocardial cells.

4.5 Presence of End-Stage Apoptosis in the LPS-Treated Heart

Apoptosis is programmed cell death, which has very characteristic end-stage markers, including fragmented DNA and a distinct morphology. Hence the reason for analysis of one or both of these in most studies of apoptosis. Fragmented nucleic DNA can be identified by TUNEL, ELISA, DNA agarose gel analysis and other methods. We chose to investigate end-stage apoptosis using TUNEL, based on its ability to detect fragmented DNA in individual cells and to allow for identification of cell type.

The heart is very resistant to LPS-induced end-stage apoptosis. Most cells within the heart did not demonstrate end-stage apoptosis as noted by the lack of positive brown stained nuclei and the presence of the counterstain, methyl green. At 24 hours post LPS an increase of 2 to 4 times the number of apoptotic myocardial cells was identified. These apoptotic cells were found in both right and left ventricle of the heart and are not present in clusters. Most of the TUNEL positive cells appear to be of non-myocardial origin. These results were not surprising for even in disease states the apoptotic index is low ^{113,114}. *In vitro* myocyte studies showing large degrees of end-stage apoptosis (10%-60%) with cytokines ^{65,110}, reactive oxygen species ^{96,115}, and nitric oxide ^{79,116} are not representative of the *in vivo* setting. The high percentage of myocyte apoptosis would likely lead to heart failure and death. Survival pathways are critical for maintaining the integrity of the heart, in agreement of the minimal amount of end-stage apoptosis present in this LPS-injected rat model. Apoptosis has been investigated in the septic patient ⁵⁸. Hotchkiss and colleagues found less than 1% apoptotic morphology in the heart which is in agreement with the amount of TUNEL positive cells detected in this

septic rat model. Other septic animal models have not investigated apoptosis in the heart

54.

The TUNEL results correlate with caspase 3 activity but not Bax and Bcl-2 protein levels. Maximum caspase 3 activity (1000 fold above control levels) is present at 24 hours post LPS, which temporally correlated with the late, rise in end-stage apoptosis. Bax and Bcl-2 have returned to control levels at this late time point when increased TUNEL positive cells are observed. These results are consistent with the interpretation that cells which have committed to late-stage apoptosis (active caspase 3) will proceed to end-stage apoptosis but those cells that have inhibited or reversed the apoptotic pathway (survival pathways, return to normal Bax and Bcl-2 levels) will survive.

Other methods for investigating DNA fragmentation, a hallmark of apoptosis, such as DNA laddering and the comet assay were not used. DNA laddering requires a large number of apoptotic cells within the tested population to see the "ladder". This may explain why some studies of the heart ^{59,61,107} confirm TUNEL or morphology data while others do not ^{58,61}. The comet assay is useful for *in vitro* studies since it test individual cells for the presence of fragmented DNA ^{65,66}. Thus in our experiment the comet assay is not feasible for whole heart. The individual myocytes collected for cytochrome C analysis would prove difficult to examine by the comet assay. These cells are collected using chemical and physical digestion, which results in 45% to 55% dead cells. Thus the isolation method used may also falsely introduced apoptotic and necrotic cells.

End-stage apoptosis is limited in this septic rat model. The lack of specific apoptotic cell location agrees with the insult being “global”. We conclude that due to the minimal number of end-stage apoptotic cells, a number of survival pathways may play an important role. At the time of maximum and significant increase in apoptotic cells the animals have largely recovered from their early physiologic response to endotoxin and display normal physical characteristics of a healthy rat. Apoptosis at this time may be due to the removal of inflammatory and severely damaged cells no longer required in the heart and thus may represent the recovery phase.

4.6 Comparison of Our Apoptotic and Survival findings with Other Cardiac Models Related to Sepsis

It is not surprising that evidence of involvement of apoptotic and survival pathways are present within this model. Although the evidence presented in this LPS-treated rat model refers to the whole heart, myocytes are included in those cell types contributing, as discussed in each section and as confirmed by the detection of some of the TUNEL positive cells to be of cardiac myocyte origin. Thus cardiac myocytes are contributing to the changes detected in these pathways. Further evidence for involvement of the cardiac myocyte *in vivo* includes *in vitro* studies related to sepsis. *In vitro* studies show that various inflammatory mediators of sepsis can induce apoptosis in cardiac myocytes, but these studies mainly focused on end-stage apoptosis and less on earlier apoptotic pathways^{65,66,110,117,118}. In fact, the pathways studied in this *in vivo* septic model have not been previously investigated in *in vitro* models.

In our septic model, LPS is used as the inducing agent. Interestingly, LPS has been shown to induce end-stage apoptosis in cultured adult cardiac myocytes via induced myocyte production of TNF α and activation of the TNFR1 receptor⁶⁶. The amount of LPS used *in vitro* was 100 ng/mL for 4 hours⁶⁶. In our septic rat model, 4 mg LPS/kg was given intraperitoneal which equates to 670 μ g/mL LPS if one assumes 60 mL of blood per kg of body weight and complete absorption. The heart may be exposed to a concentration of ≥ 100 ng/mL for some time although whether this continues for 4 hours is unknown due to the body's metabolism. It does however, suggest that the possibility may exist *in vivo*. The 100 ng/mL LPS was associated with TNF α production by the cardiac myocyte to levels of ~ 500 pg/mL. Higher concentrations of TNF α are observed in many animal models after LPS injection. The fraction of apoptotic cardiac myocytes present after a 4 hour incubation with 100 ng/mL LPS in serum free media was $\sim 18\%$ compared with $\sim 4\%$ in control cells. This level of end-stage apoptosis was not seen *in vivo*. The *in vitro* model is very unrepresentative of *in vivo* conditions in many ways including the presence of serum and the influence by pro-survival pathways. Our study extends this *in vitro* study by suggesting specific apoptotic pathways that are activated in the heart as the result of LPS.

LPS is a well known inducer of TNF α production. *In vitro* TNF α (4 nM, 68 pg/mL) challenged adult cardiac myocytes for 18 hours showed $\sim 60\%$ apoptosis as measured by the comet assay⁶⁵. A minimum time of 12 hours was required to detect any significant increase in cardiac myocyte apoptosis⁶⁵. The level and time presence of TNF α in the

heart of our septic model is unknown. However, a study by Shames and colleagues also using a rat LPS model, measured maximum TNF α level at 2 hours following LPS injection, which then decline to control levels by 4 hours ¹¹⁹. Maximum TNF α was 32 pg per mg of cardiac tissue ¹¹⁹. Once again converting to per mL of blood using 60 mL per kg we have a concentration of 533 ng/mL. Thus the level of TNF α used by Krown would be present in our rat model. Once again end-stage apoptosis *in vitro* results are different from *in vivo*. The apoptotic inducing capacity of TNF α was shown to occur via TNFR1 receptor by use of antibodies to the receptor and by using sphingosine, a known product of TNFR1 ⁶⁵. This study also supports our observation of activation of apoptotic and survival studies in our LPS-treated rat model.

In vitro studies have also shown TNF α ability to induce apoptosis in endothelial cells and in smooth muscle cells ^{111,120}.

Other inflammatory mediators of sepsis, including nitric oxide and reactive oxygen species, have been found to induce apoptosis in many cell types including myocytes ^{117,118}. Apoptosis by nitric oxide is caused from the calcium independent iNOS ¹¹⁶. Adult cardiac myocytes challenged with SNAP (1 mM, a nitric oxide donor) will induce 40% of cardiac myocytes to undergo apoptosis within 4 hours. Hemoglobin, which scavenges nitric oxide, can prevent the increase in apoptosis caused by SNAP at 4 hours but is less successful at preventing apoptosis at 8 hours (42% SNAP vs 30% SNAP + hemoglobin vs 13% control). If nitric oxide is not completely neutralized then nitric oxide directly or indirectly can still activate apoptosis. Survival pathways would also be

activated as suggested by the lack of 100% cell death *in vitro* and *in vivo*. Cytokines can also cause end-stage apoptosis by inducing the downstream activator nitric oxide ¹¹⁶.

During sepsis the heart responds less to β -agonist drugs as compared with a healthy heart ¹²¹. Interestingly the β -adrenergic receptor stimulation has been shown to cause apoptosis in adult and neonatal myocytes ^{122,123}. The cardiac cell contains two types of β -adrenergic receptors, β_1 and β_2 ¹²². Communal and colleagues showed that only β_1 , and not β_2 , receptor stimulation will cause apoptosis ¹²². The β_1 receptor promotes apoptosis by inducing cAMP. Further confirmation that the β adrenergic receptor contributes to the induction of apoptosis comes from the $G_{s\alpha}$ transgenic mouse mice ¹²⁴. The $G_{s\alpha}$ transgenic mouse over-expresses $G_{s\alpha}$ the immediate downstream protein of the β receptor. The $G_{s\alpha}$ transgenic mouse presents more apoptosis than control mice when stimulated via the β receptor ¹²⁴. In contrast, the α adrenergic receptor; promotes cardiac myocyte survival ¹²³. Whether the decreased cardiac response to β -adrenergic agonists during human sepsis has an impact on cardiac myocyte apoptosis during sepsis is unknown.

Calcium regulation is disrupted during sepsis ^{28,125}. Cytosolic calcium concentrations increase during sepsis as the result of a less efficient Na^+-Ca^{2+} exchanger in the sarcolemma and an impaired Ca^{2+} -ATPase pump on the sarcolemma ^{28,125}. Increased cytoplasmic calcium concentrations have been causally connected with apoptosis ¹²⁶. Increased cytosolic calcium may activate key apoptotic pathways such as the effector

machinery. Proteases (ex. laminin protease), and endonucleases (ex. DNaseI) are calcium sensitive ¹²⁶. The phosphatidylserine “flip” characteristic of apoptosis is also calcium sensitive. Hence, increased cytosolic calcium is one more contributing factor to the activation of apoptotic pathways within the septic heart and specifically within the cardiac myocyte.

Activation of apoptotic pathways occurs in the heart and in cardiac myocytes. Survival pathways are also important, as shown indirectly by the low percentage of end-stage apoptosis *in vivo* and lack of 100% death rate *in vitro*. The pathways investigated in this septic rat model are the result of one or more of the above inducers. The pathways investigated (Bax/Bcl-2, cytochrome C, caspase) are unlikely to be the only pathways involved. Further investigation into other pathways is necessary (ex. Bid, p53). Our findings extend *in vitro* findings to *in vivo*, showing a more complex response and we identified some of the pathways involved.

4.7 Myocardial Function in the LPS-Treated Rat Model

Sepsis is accompanied by myocardial dysfunction. Known contributing factors include TNF α and nitric oxide. Activation of apoptotic pathways could conceivably contribute to this myocardial dysfunction. Thus we investigated the correlation between activation of these apoptotic and survival pathways with myocardial function. Myocardial function was determined in isolated cardiac myocytes by measuring their percent fractional shortening. Fractional shortening has been shown to correlate with *in vivo* heart function as determined by echo ¹²⁷. Fractional shortening has also been proven to detect changes

in cardiac contractility caused by *in vitro* challenge²⁴. Hence, fractional shortening on isolated cardiac myocytes taken from *in vivo* LPS-treated rats was measured.

We found that intraperitoneal LPS injection caused myocardial dysfunction in the rat. LPS maximally depressed myocyte contraction by 29% at six hours post LPS treatment. Half of this decrease recovered by 12 hours post LPS treatment and remained at 24 hours post LPS. These results are in agreement with other investigators using a variety of animal models that have demonstrated myocardial dysfunction after endotoxin infusion^{21,128-131}. Depression of cardiac contractility in this LPS rat model is similar to that seen with other models measuring Emax (29% fractional shortening versus 40% Emax^{21,128}. To illustrate the relationship between fractional shortening and a volume-based measured such as Emax we note that for a sphere a 25% fractional shortening of diameter translates into a 58% reduction in volume ejection at the same pressure. Most studies do not proceed past 6 hours of LPS exposure. By 24 hours post LPS injection, the rat's physical appearance is normal yet cardiac contractility was still suppressed. The exact cause of this incomplete recovery is unknown but may be related to chronic studies where recovery occurs over a period of days.

The decrease in cardiac function present in this LPS-treated rat model was temporally more closely correlated with changes in Bax and Bcl-2 expression and decreased mitochondrial cytochrome C rather than with the presence of end-stage apoptosis. At the time of maximum cardiac depression end-stage apoptosis as determined by TUNEL had not risen above control levels. TUNEL indicated a slight increase in apoptotic cells at 24

hours post LPS compared to 6 and 12 hours while contractility improved. Recovery in contractility was seen at 12 hours with no corresponding change in TUNEL results. Thus, it appears less likely that end-stage apoptosis was associated with a depressed cardiac function. Myocyte apoptosis however has been associated with myocardial dysfunction in a number of clinical heart disease states such as ischemia-reperfusion, myocardial infarction, and chronic heart failure ^{59,62,113,132}. Ventricular dysfunction in these studies likely required apoptosis of many more cardiac myocytes than we observed in this relatively short sepsis study. This does not rule out the relationship between heart dysfunction and apoptosis. For instance, increased myocyte apoptosis has been associated with age and ventricular dysfunction ⁶³. Furthermore, failing ventricles in spontaneously hypertensive rats show greater than four times the number of apoptotic cardiomyocytes than that seen in non-failing hypertensive rat ventricles ⁶⁴. Loss of cardiac myocytes probably contribute to heart dysfunction because without replacement of these cells fewer cells must maintain heart function. Yet apoptotic pathways may be linked to cardiac myocyte dysfunction in other ways.

Evidence that apoptotic pathways themselves, and not necessarily end-stage apoptosis, are correlated with myocardial dysfunction is taken from the data collected at the time of maximum cardiac dysfunction. Maximum decrease in fractional shortening observed following LPS injection was more closely correlated with mitochondria-related apoptotic events (decrease in Bax and Bcl-2 protein, increase Bcl-2 mRNA, and loss of mitochondrial cytochrome C) than with the evidence of minimal end-stage apoptosis at 24 hours. Thus, it is interesting to speculate that the effects of apoptotic pathways on

mitochondrial function may be more important than end-stage apoptosis in contributing to myocardial dysfunction of sepsis. Possible interactions between mitochondrial function and apoptosis under septic conditions include PKC and the mitochondrial respiratory complex I. TNF α is known to activate sphingosine prior to inducing apoptosis in cultured adult cardiac myocytes⁶⁵. Sphingosine is a known inhibitor of PKC⁶⁵. Without operational PKC, myocyte contraction can decrease (Figure 1) and Bcl-2 activity may decrease due to a change in Bcl-2 phosphorylation state⁶⁵. Sphingosine-1-phosphate, a known product of sphingosine, has been shown to increase Bax protein levels in Hep3B human hepatoma cells¹³³. In a cecal ligation and puncture septic rat model, PKC activity was increased 9 hours following surgery but was within control levels 18 hours following surgery¹³⁴. These results may argue against the proposed interaction between mitochondria and apoptosis. However, another report suggests that cecal ligation and puncture may not be a good model for study septic myocardial dysfunction because myocardial dysfunction does not always occur¹⁰². In a septic baboon model caused by the infusion of live *E. coli* bacteria, the activity of mitochondrial respiratory complex I was decreased⁷⁵. Inhibition of the mitochondrial respiratory complex I, but not II, in ML-1a cells using rotenone (MRC complex I inhibitor) and cycloheximide (protein synthase inhibitor) has been linked with release of cytochrome C and DNA fragmentation¹³⁵. Other possible interactions may exist between the mitochondria, apoptosis, and cardiac dysfunction. Speculatively, apoptotic regulators (i.e. the Bcl-2 family) may interact with known damaged contractile apparatus present in sepsis like the ryanodine receptor²⁶, PKA¹³⁶, Ca²⁺-ATPase^{28,125}, Na⁺-

Ca²⁺ exchanger²⁷. Mitochondrial involvement in apoptosis can be reversible¹³⁷! Human osteosaroma cells treated with CCCP cause the mitochondria to depolarize, resulting in PT pore opening. This event is reversible if the treatment is less than 6 hours¹³⁷. The possibility of mitochondria dysfunction caused by a reversible apoptotic mechanism lends support to the hypothesis that apoptosis pathways involving the mitochondria may contribute to myocardial dysfunction. In sepsis, myocardial dysfunction is reversible, hence the importance of this possibility in the apoptotic mitochondria.

Intraperitoneal LPS injection induces myocardial dysfunction in rat cardiac myocytes isolated from the heart 6 hours later. The maximal decrease in percent fractional shortening correlates well with the time course of activation of apoptotic pathways specifically related to mitochondria. Late-stage and end-stage apoptosis are not temporally closely correlated with the decrease in percent fractional shortening of isolated rat cardiac myocytes.

4.8 *In vitro* Analysis of Cardiac Myocytes for Investigating the Link between Apoptosis and Cardiac dysfunction.

To further establish a link between activation of apoptotic pathways and myocardial dysfunction we extended the study to include *in vitro* challenge of cardiac myocytes with agents reported in the literature as being capable of inducing apoptosis in this cell type.

The first step to investigating this relationship was to establish an *in vitro* cardiac myocyte apoptotic model. A variety of agents were tested.

Establishing an *in vitro* cardiac myocyte apoptosis model proved difficult. The *in vitro* analysis was carried out on non-dividing adult cardiac myocytes. A successful isolation would result in $5-7 \times 10^5$ cells. Of this cell population 30%-40% consisted of dead myocytes. 24 well plates were chosen to establish the model because it would allow for multiple testing groups and provided cells for more than one mode of analysis. One 24 well plate requires $\sim 5 \times 10^5$ cells to plate cells at 20 000 per well. Removing supernatant and refeeding at 90 minutes eliminated more of the dead cells because dead cells do not adhere to the culture plate, but not completely. The resulting number of cardiac myocytes per well was approximately 60%-70% of the original number plated. After challenge with apoptosis-inducing agents and trypsinization to detach adherent viable cells from the plate, the cells were divided into 1 to 3 groups. Most cells were used for TUNEL analysis and of these $\sim 30\%$ of the cells were lost during the fixing process. The end result is few cells per test, and in some cases, multiple tests of the same group had to be pooled, thus decreasing the total number of tests.

Testing of several reported apoptosis inducing agents was tried on isolated cardiac myocytes. Cardiac myocytes challenged with $\text{TNF}\alpha$ appeared to increase the number of apoptotic cells compared with control but this trend was non-significant (Figure 13). Morphological studies likewise did not consistently demonstrate end-stage apoptosis and therefore did not provide support for the *in vitro* TUNEL data. Krown and colleagues

reported that a 18 hour challenge with 68 pg/mL of TNF α was capable of inducing adult cardiac myocyte apoptosis in 47.6%, as determined by the comet assay, and in 32.5% as shown by TUNEL⁶⁵. This was a much greater effect than what we observed with the 1-200 ng/mL TNF α tested here. Krown also reported that 10 μ M sphingosine for 18 hours induced 95% apoptosis⁶⁵. Sphingosine (10 μ M) in this study resulted in only 10% apoptosis as determined by TUNEL with no confirmation by morphology. Krown's study did involve adult rat cardiac myocytes but the species of rat was not reported, which may have been different from the one used in this study. Alternatively, our cardiac myocyte isolation procedure may differ and may explain some of the discrepancies. IL-1 β was also tested by itself and in combination with TNF α (Table 2). Levels of apoptotic cells after challenge with IL-1 β for 24 hours were low but slightly higher than the control. This is in agreement with studies of neonatal cardiac myocytes that show no difference in apoptotic levels with 5 ng/mL IL-1 β within the first 24 hours¹¹⁰. IL-1 β does induce 45% apoptosis in neonatal cardiac myocytes if present for 120 hours¹¹⁰. IL-1 β in conjugation with TNF α is known to act synergistically²⁰ in inducing myocardial dysfunction in isolated cardiac myocytes; however, even this combination did not result in much apoptosis (Table 2). In fact 5 ng/mL of both IL-1 β / TNF α gave a higher percentage of TUNEL positive cells than both cytokines at 10 ng/mL and not more than IL-1 β at 5ng/mL. Staurosporine has been shown to cause apoptosis without the need for de novo protein synthesis¹⁰⁸. Staurosporine at 1 μ M and 2 μ M was used to challenge cardiac myocytes for 24 hours. Both concentrations did not result in an increase in cardiac myocyte apoptosis. Staurosporine at 1.0 μ M has been shown to induce 55%

apoptosis in neonatal cardiac myocytes within 24 hours. Adult cardiac myocytes appear more resistant. Fas, an apoptosis inducer in many cell types, did not induce apoptosis in the adult cardiac myocyte. Neonatal chick myocytes can undergo apoptosis in the presence of camptothecin, a topoisomerase inhibitor, within 6-8 hours (Drs. N. Reiner and V. Durino (UBC), personal communications). This was not the case for adult rat cardiac myocytes. Adult Sprague Dawley rat cardiac myocytes proved resistant to the tested apoptosis inducing agents. It's not unusual for apoptosis inducing agents to work in neonatal and not adult. However, it was anticipated that the TNF α or sphingosine would have shown an effect on the adult cardiac myocyte. Either induction of apoptosis is strain specific or there existed a technical problem. Alternatively, the presence of an additional cell type may be needed to successfully cause end-stage apoptosis in our cardiac myocyte cell culture system, thereby representing the *in vivo* situation more closely.

Functional measurement of the *in vitro* challenged cardiac myocytes was determined by fractional shortening. Fractional shortening of adult cardiac myocytes after 24 hours of culture was not different between control and any of the treated groups. The ineffectiveness of TNF α on the cardiac myocyte is in agreement with previous studies from our laboratory that have shown the necessary presence of macrophages ²⁴.

Sphingosine, staurosporine, Fas, and camptothecin have not been investigated for their action on myocardial dysfunction. The preliminary findings of these agents in the model system tested here suggested that they do not negatively effect myocardial function. These findings need to be further investigated due to the limited analysis in this study.

Due to the limited percentage of potential, though not confirmed, apoptotic myocytes as compared with control samples and those percentages reported in the literature, the *in vitro* study was not pursued further.

4.9 Pitfalls and Future Directions

Analysis of apoptotic and survival pathways was achieved for the whole LPS-exposed heart. The chief limitation of these studies is that the contribution by specific cell types is uncertain. TUNEL analysis identified cells that achieved end-stage apoptosis. These TUNEL positive cells contributed to the experimental findings but may not represent all contributing cell types. This is particularly true in that positive TUNEL staining was not the apoptosis-associated measure that correlated with decreased fractional shortening.

With only partial identification of those cell types involved, we are unable to speculate as to the percent contribution by each cell type. Thus results should not be applied to any specific cell type. For example, the ratio of Bax to Bcl-2 was determined for the whole heart and therefore unlikely to represent every cell type in the heart. Caspase 3 activity is also for the whole heart and as explained previously many cell types within the heart are known to activate caspase 3 in response to either LPS or cytokines such as TNF α .

This septic model represents only the acute stages of the disease and therefore was only studied during the first 24 hours. Many events, however, were still occurring at the 24 hour time point. Bax and Bcl-2 protein levels were still changing at 24 hours, making it unclear if these levels will continue changing or will stabilize at future time points. Both

caspase 3 activity and end-stage apoptosis were also on the rise at 24 hours. Heart function had stabilized but had not reached control levels at 24 hours post LPS. Thus the physical outcome past 24 hours is unknown due to these changing events. It would be useful to continue the study until the events reached control levels or had stabilized to a new homeostasis. At 24 hours post LPS, the physical characteristic of the rat was that of a healthy rat, thus giving the appearance of recovery. This however, may not be true due to the changing status of each of the above events.

To aid in future apoptotic studies, a larger LPS dose could be given to produce a larger apoptotic signal. A higher dosage is possible because zero mortality was achieved with the 4 mg/kg dosage used in this study.

This LPS rat model is only an acute model of sepsis and therefore does not mimic the true continuous infection of sepsis. Cecal ligation and puncture perhaps offers a better continuous infectious model but has shown to not to have the same depressant effects on the heart as LPS 102,128-130.

To further connect activation of apoptotic pathways with myocardial dysfunction an *in vitro* model was attempted. The *in vitro* study identified difficulties in inducing apoptosis in adult cardiac myocytes. Further work at establishing an apoptotic cardiac myocyte *in vitro* model is necessary. Perhaps further investigation into the effect of TNF α on cardiac myocytes would be useful. Another problem with the *in vitro* study was the lack of cells. Possibilities to help eliminate this problem include use of more rats or use of a

cell line. Currently there exist two cardiac myocyte cell lines, one rat and one human.

The difficulties with these cell lines are 1) they are neonatal and 2) do they truly represent a cardiac myocyte? An alternative, but again not cell-specific, method to study the correlation between apoptosis and cardiac function is to block the apoptotic pathways *in vivo*.

4.10 Conclusion

Involvement of apoptotic pathways has been documented in the heart following an LPS injection in rats. Initially both survival and apoptotic pathways are activated and associated with a potential loss of mitochondrial cytochrome C in cardiac myocytes, followed by increasing caspase 3 activity, and a small degree of end-stage apoptosis by 24 hours. Apoptosis was not selective to any particular region of the heart. Myocardial dysfunction was present at all time points as measured in this acute LPS rat model with maximal dysfunction occurring at 6 hours following LPS injection. We conclude that involvement of apoptotic and survival pathways occurs in the heart during a septic inflammatory response. Activation of these apoptotic pathways, specifically those related to mitochondria involvement, temporally correlate with myocardial dysfunction.

CHAPTER 5: REFERENCES

1. Sands K. E., D. W. Bates, P. N. Lanken, P. S. Graman, P. L. Hibberd, K. L. Kahn, J. Parsonnet, R. Panzer, E. J. Orav, D. R. Snyderman. Epidemiology of sepsis syndrome in 8 academic medical centers. Academic Medical Center Consortium Sepsis Project Working Group. *JAMA*.278:234-240, 1997.
2. Carleton S. C. The cardiovascular effects of sepsis. *Cardiol. Clin.*13:249-256, 1995.
3. Balk R. A., R. C. Bone. The septic syndrome. Definition and clinical implications. *Crit. Care Clin.*5:1-8, 1989.
4. Birdsall H. H., D. M. Green, J. Trial, K. A. Youker, A. R. Burns, C. R. MacKay, G. J. LaRosa, H. K. Hawkins, C. W. Smith, L. H. Michael, M. L. Entman, R. D. Rossen. Complement C5a, TGF-beta 1, and MCP-1, in sequence, induce migration of monocytes into ischemic canine myocardium within the first one to five hours after reperfusion. *Circulation*.95:684-692, 1997.
5. Haeney M. R. The role of the complement cascade in sepsis. *J. Antimicrob. Chem.*41:41-46, 1998.
6. van der Poll T., H. R. Buller, H. ten Cate, C. H. Wortel, K. A. Bauer, S. J. van Deventer, C. E. Hack, H. P. Sauerwein, R. D. Rosenberg, J. W. ten Cate. Activation of coagulation after administration of tumor necrosis factor to normal subjects. *N. Eng. J. Med.*322:1622-1627, 1990.
7. Meyer T. A., J. Wang, G. M. Tiao, C. K. Ogle, J. E. Fischer, P. O. Hasselgren. Sepsis and endotoxemia stimulate intestinal interleukin-6 production. *Surgery*.118:336-342, 1995.

8. Kasai T., K. Inada, T. Takakuwa, Y. Yamada, Y. Inoue, T. Shimamura, S. Taniguchi, S. Sato, G. Wakabayashi, S. Endo. Anti-inflammatory cytokine levels in patients with septic shock. *Res Commun Mol Pathol Pharmacol*.98:34-42, 1997.
9. Opal S. M., J. Cohen. Clinical gram-positive sepsis: does it fundamentally differ from gram-negative bacterial sepsis? *Crit Care Med*.27:1608-1616, 1999.
10. Barber A., T. Shires, G. Shires. Shock. In: SI S, ed. *Principles of Surgery*. 7th ed. New York: McGraw-Hill Health Professions Divison; 1999:101-122.
11. Ziegler E. J., C. J. Fisher, Jr., C. L. Sprung, R. C. Straube, J. C. Sadoff, G. E. Foulke, C. H. Wortel, M. P. Fink, R. P. Dellinger, N. N. Teng, et al. Treatment of gram-negative bacteremia and septic shock with HA-1A human monoclonal antibody against endotoxin. A randomized, double-blind, placebo-controlled trial. The HA-1A Sepsis Study Group. *N. Eng. J. Med*.324:429-436, 1991.
12. Bone R. C., R. A. Balk, A. M. Fein, T. M. Perl, R. P. Wenzel, H. D. Reines, R. W. Quenzer, T. J. Iberti, N. Macintyre, R. M. Schein. A second large controlled clinical study of E5, a monoclonal antibody to endotoxin: results of a prospective, multicenter, randomized, controlled trial. The E5 Sepsis Study Group [published erratum appears in Crit Care Med 1995 Sep;23(9):1616]. *Crit. Care Med*.23:994-1006, 1995.
13. Read R. C. Experimental therapies for sepsis directed against tumour necrosis factor. *J. Antimicrob. Chem*.41:65-69, 1998.
14. Horn K. D. Evolving strategies in the treatment of sepsis and systemic inflammatory response syndrome (SIRS). *Qjm*.91:265-277, 1998.

15. Walley K. R. Mechanisms of Decreased Cardiac Function in Sepsis. In: Vincent JL, ed. *Yearbook of Intensive Care and Emergency Medicine*: Springer-Verlag Berlin Heidelberg; 1997:243-255.
16. Parker M. M., A. F. Suffredini, C. Natanson, F. P. Ognibene, J. H. Shelhamer, J. E. Parrillo. Responses of left ventricular function in survivors and nonsurvivors of septic shock. *J. Crit. Care*.4:19-25, 1989.
17. Parrillo J. E., C. Burch, J. H. Shelhamer, M. M. Parker, C. Natanson, W. Schuette. A circulating myocardial depressant substance in humans with septic shock. Septic shock patients with a reduced ejection fraction have a circulating factor that depresses in vitro myocardial cell performance. *J. Clin. Invest*.76:1539-1553, 1985.
18. Carli A., M. C. Auclair, C. Benassayag, E. Nunez. Evidence for an early lipid soluble cardiodepressant factor in rat serum after a sublethal dose of endotoxin. *Circ. Shock*.8:301-312, 1981.
19. Gomez A., R. Wang, H. Unruh, R. B. Light, D. Bose, T. Chau, E. Correa, S. Mink. hemofiltration reverses left ventricular dysfunction during sepsis in dogs. *Anesthesiology*.73:671-685, 1990.
20. Kumar A., V. Thota, L. Dee, J. Olson, E. Uretz, J. E. Parrillo. Tumor necrosis factor alpha and interleukin 1beta are responsible for in vitro myocardial cell depression induced by human septic shock serum. *J. Exp. Med*.183:949-958, 1996.
21. Herbertson M. J., H. A. Werner, C. M. Goddard, J. A. Russell, A. Wheeler, R. Coxon, K. R. Walley. Anti-tumor necrosis factor-alpha prevents decreased

- ventricular contractility in endotoxemic pigs. *Am. J. Respir. Crit. Care Med.* 152:480-488, 1995.
22. Eichenholz P. W., P. Q. Eichacker, W. D. Hoffman, S. M. Banks, J. E. Parrillo, R. L. Danner, C. Natanson. Tumor necrosis factor challenges in canines: patterns of cardiovascular dysfunction. *Am. J. Physiol.* 263:H668-675, 1992.
 23. Kumar A., R. Brar, P. Wang, L. Dee, G. Skorupa, F. Khadour, R. Schulz, J. E. Parrillo. Role of nitric oxide and cGMP in human septic serum-induced depression of cardiac myocyte contractility. *Am. J. Physiol.* 276:R265-276, 1999.
 24. Simms M. G., K. R. Walley. Activated macrophages decrease rat cardiac myocyte contractility: importance of ICAM-1-dependent adhesion. *Am J Physiol.* 277:H253-260, 1999.
 25. Finkel M. S., C. V. Oddis, T. D. Jacob, S. C. Watkins, B. G. Hattler, R. L. Simmons. Negative inotropic effects of cytokines on the heart mediated by nitric oxide. *Science.* 257:387-389, 1992.
 26. Wu L. L., M. S. Liu. Altered ryanodine receptor of canine cardiac sarcoplasmic reticulum and its underlying mechanism in endotoxin shock. *J Surg Res.* 53:82-90, 1992.
 27. Liu M. S., Y. T. Xuan. Mechanisms of endotoxin-induced impairment in Na⁺-Ca²⁺ exchange in canine myocardium. *Am J Physiol.* 251:R1078-1085, 1986.
 28. Liu M. S., L. L. Wu. Heart sarcolemmal Ca²⁺ transport in endotoxin shock: II. Mechanism of impairment in ATP-dependent Ca²⁺ transport. *Mol Cell Biochem.* 112:135-142, 1992.

29. Carpati C. M., M. E. Astiz, E. C. Rackow. Mechanisms and management of myocardial dysfunction in septic shock. *Crit Care Med.*27:231-232, 1999.
30. Tao S., T. M. McKenna. In vitro endotoxin exposure induces contractile dysfunction in adult rat cardiac myocytes. *Am. J. Physiol.*267:H1745-1752, 1994.
31. Schulz R., D. L. Panas, R. Catena, S. Moncada, P. M. Olley, G. D. Lopaschuk. The role of nitric oxide in cardiac depression induced by interleukin-1 beta and tumour necrosis factor-alpha. *Br J Pharmacol.*114:27-34, 1995.
32. Haunstetter A., S. Izumo. Apoptosis: basic mechanisms and implications for cardiovascular disease. *Circ. Res.*82:1111-1129, 1998.
33. Kerr J. F., A. H. Wyllie, A. R. Currie. Apoptosis: a basic biological phenomenon with wide-ranging implications in tissue kinetics. *Br J Cancer.*26:239-257, 1972.
34. Allen R. T., W. J. Hunter, 3rd, D. K. Agrawal. Morphological and biochemical characterization and analysis of apoptosis. *J. Pharmacol. Toxicol. Methods.*37:215-228, 1997.
35. Colucci W. S. Apoptosis in the heart [editorial; comment] [published erratum appears in N Engl J Med 1997 Apr 24;336(17):1267]. *N Engl J Med.*335:1224-1226, 1996.
36. Kroemer G. The proto-oncogene Bcl-2 and its role in regulating apoptosis. *Nat. Med.*3:614-620, 1997.
37. Condorelli G., C. Morisco, G. Stassi, A. Notte, F. Farina, G. Sgaramella, A. de Rienzo, R. Roncarati, B. Trimarco, G. Lembo. Increased cardiomyocyte apoptosis and changes in proapoptotic and antiapoptotic genes bax and bcl-2 during left

- ventricular adaptations to chronic pressure overload in the rat.
Circulation.99:3071-3078, 1999.
38. Misao J., Y. Hayakawa, M. Ohno, S. Kato, T. Fujiwara, H. Fujiwara. Expression of bcl-2 protein, an inhibitor of apoptosis, and Bax, an accelerator of apoptosis, in ventricular myocytes of human hearts with myocardial infarction.
Circulation.94:1506-1512, 1996.
 39. de Moissac D., H. Zheng, L. A. Kirshenbaum. Linkage of the BH4 domain of Bcl-2 and the nuclear factor kappaB signaling pathway for suppression of apoptosis [published erratum appears in J Biol Chem 2000 Jan 28;275(4):3016]. *J Biol Chem*.274:29505-29509, 1999.
 40. Green D., G. Kroemer. The central executioners of apoptosis: caspases or mitochondria? *Trends. Cell.Biol*.8:267-271, 1998.
 41. Goping I. S., A. Gross, J. N. Lavoie, M. Nguyen, R. Jemmerson, K. Roth, S. J. Korsmeyer, G. C. Shore. Regulated targeting of BAX to mitochondria. *J. Cell Biol*.143:207-215, 1998.
 42. Fortuno M. A., G. Zalba, S. Ravassa, E. D'Elom, F. J. Beaumont, A. Fortuno, J. Diez. p53-mediated upregulation of BAX gene transcription is not involved in Bax-alpha protein overexpression in the left ventricle of spontaneously hypertensive rats. *Hypertension*.33:1348-1352, 1999.
 43. Cai J., J. Yang, D. P. Jones. Mitochondrial control of apoptosis: the role of cytochrome c. *Biochem. Biophys. Acta*.1366:139-149, 1998.
 44. Green D. R., J. C. Reed. Mitochondria and apoptosis. *Science*.281:1309-1312, 1998.

45. Susin S. A., N. Zamzami, G. Kroemer. Mitochondria as regulators of apoptosis: doubt no more. *Biochim. Biophys. Acta.*1366:151-165, 1998.
46. Finucane D. M., E. Bossy-Wetzel, N. J. Waterhouse, T. G. Cotter, D. R. Green. Bax-induced caspase activation and apoptosis via cytochrome c release from mitochondria is inhibitable by Bcl-xL. *J. Biol. Chem.*274:2225-2233, 1999.
47. Susin S. A., H. K. Lorenzo, N. Zamzami, I. Marzo, C. Brenner, N. Larochette, M. C. Prevost, P. M. Alzari, G. Kroemer. Mitochondrial release of caspase-2 and -9 during the apoptotic process. *J. Exp. Med.*189:381-394, 1999.
48. Ayala A., Y. Xin Xu, C. A. Ayala, D. E. Sonefeld, S. M. Karr, T. A. Evans, I. H. Chaudry. Increased mucosal B-lymphocyte apoptosis during polymicrobial sepsis is a Fas ligand but not an endotoxin-mediated process. *Blood.*91:1362-1372, 1998.
49. Chung C. S., Y. X. Xu, W. Wang, I. H. Chaudry, A. Ayala. Is Fas ligand or endotoxin responsible for mucosal lymphocyte apoptosis in sepsis? *Arch. Surg.*133:1213-1220, 1998.
50. Hotchkiss R. S., P. E. Swanson, J. P. Cobb, A. Jacobson, T. G. Buchman, I. E. Karl. Apoptosis in lymphoid and parenchymal cells during sepsis: findings in normal and T- and B-cell-deficient mice. *Crit. Care Med.*25:1298-1307, 1997.
51. Williams T. E., A. Ayala, I. H. Chaudry. Inducible macrophage apoptosis following sepsis is mediated by cysteine protease activation and nitric oxide release. *J. Surg. Res.*70:113-118, 1997.
52. Ayala A., M. A. Urbanich, C. D. Herdon, I. H. Chaudry. Is sepsis-induced apoptosis associated with macrophage dysfunction? *J Trauma.*40:568-573; discussion 573-564, 1996.

53. Barke R. A., S. Roy, R. B. Chapin, R. Charboneau. The role of programmed cell death (apoptosis) in thymic involution following sepsis. *Arch. Surg.* 129:1256-1261; discussion 1261-1252, 1994.
54. Haendeler J., U. K. Messmer, B. Brune, E. Neugebauer, S. Dimmeler. Endotoxic shock leads to apoptosis in vivo and reduces Bcl-2. *Shock* 6:405-409, 1996.
55. Ayala A., T. A. Evans, I. H. Chaudry. Does hepatocellular injury in sepsis involve apoptosis? *J. Surg. Res.* 76:165-173, 1998.
56. Ertel W., M. Keel, M. Infanger, U. Ungethum, U. Steckholzer, O. Trentz. Circulating mediators in serum of injured patients with septic complications inhibit neutrophil apoptosis through up-regulation of protein-tyrosine phosphorylation. *J Trauma* 44:767-775; discussion 775-766, 1998.
57. Keel M., U. Ungethum, U. Steckholzer, E. Niederer, T. Hartung, O. Trentz, W. Ertel. Interleukin-10 counterregulates proinflammatory cytokine-induced inhibition of neutrophil apoptosis during severe sepsis. *Blood* 90:3356-3363, 1997.
58. Hotchkiss R. S., P. E. Swanson, B. D. Freeman, K. W. Tinsley, J. P. Cobb, G. M. Matuschak, T. G. Buchman, I. E. Karl. Apoptotic cell death in patients with sepsis, shock, and multiple organ dysfunction. *Crit Care Med* 27:1230-1251, 1999.
59. Olivetti G., R. Abbi, F. Quaini, J. Kajstura, W. Cheng, J. A. Nitahara, E. Quaini, C. Di Loreto, C. A. Beltrami, S. Krajewski, J. C. Reed, P. Anversa. Apoptosis in the failing human heart. *N. Engl. J. Med.* 336:1131-1141, 1997.

60. Kajstura J., M. Mansukhani, W. Cheng, K. Reiss, S. Krajewski, J. C. Reed, F. Quaini, E. H. Sonnenblick, P. Anversa. Programmed cell death and expression of the protooncogene bcl-2 in myocytes during postnatal maturation of the heart. *Exp. Cell Res.*219:110-121, 1995.
61. Bialik S., D. L. Geenen, I. E. Sasson, R. Cheng, J. W. Horner, S. M. Evans, E. M. Lord, C. J. Koch, R. N. Kitsis. Myocyte apoptosis during acute myocardial infarction in the mouse localizes to hypoxic regions but occurs independently of p53. *J. Clin. Invest.*100:1363-1372, 1997.
62. Gottlieb R. A., K. O. Burleson, R. A. Kloner, B. M. Babior, R. L. Engler. Reperfusion injury induces apoptosis in rabbit cardiomyocytes. *J. Clin. Invest.*94:1621-1628, 1994.
63. Kajstura J., W. Cheng, R. Sarangarajan, P. Li, B. Li, J. A. Nitahara, S. Chapnick, K. Reiss, G. Olivetti, P. Anversa. Necrotic and apoptotic myocyte cell death in the aging heart of Fischer 344 rats. *Am. J. Physiol.*271:H1215-1228, 1996.
64. Li Z., O. H. Bing, X. Long, K. G. Robinson, E. G. Lakatta. Increased cardiomyocyte apoptosis during the transition to heart failure in the spontaneously hypertensive rat. *Am. J. Physiol.*272:H2313-2319, 1997.
65. Krown K. A., M. T. Page, C. Nguyen, D. Zechner, V. Gutierrez, K. L. Comstock, C. C. Glembotski, P. J. Quintana, R. A. Sabbadini. Tumor necrosis factor alpha-induced apoptosis in cardiac myocytes. Involvement of the sphingolipid signaling cascade in cardiac cell death. *J. Clin. Invest.*98:2854-2865, 1996.
66. Comstock K. L., K. A. Krown, M. T. Page, D. Martin, P. Ho, M. Pedraza, E. N. Castro, N. Nakajima, C. C. Glembotski, P. J. Quintana, R. A. Sabbadini. LPS-

- induced TNF- α release from and apoptosis in rat cardiomyocytes: obligatory role for CD14 in mediating the LPS response. *J Mol Cell Cardiol.*30:2761-2775, 1998.
67. Parratt J. R. Nitric oxide in sepsis and endotoxaemia. *J. Antimicrob. Chemother.*41:31-39, 1998.
 68. Goddard C. M., M. F. Allard, J. C. Hogg, M. J. Herbertson, K. R. Walley. Prolonged leukocyte transit time in coronary microcirculation of endotoxemic pigs. *Am. J. Physiol.*269:H1389-1397, 1995.
 69. Brune B., A. von Knethen, K. B. Sandau. Nitric oxide and its role in apoptosis. *Eur. J. Pharmacol.*351:261-272, 1998.
 70. Dimmeler S., A. M. Zeiher. Nitric oxide and apoptosis: another paradigm for the double-edged role of nitric oxide. *Nitric Oxide.*1:275-281, 1997.
 71. Dakhama A., N. Chan, H. Ahmad, A. Bramley, T. Vitalis, R. Hegelle. Usefulness of bronchoalveolar lavage for diagnosis of acute and persistent respiratory syncytial virus lung infections in guinea pigs. *Pediatr. Pulmonol.*26:396-404, 1998.
 72. Granville D., J. Levy, D. Hunt. Photodynamic therapy induces caspase-3 activation in HL-60 cells. *Cell Death Differ.*4:623-629, 1997.
 73. Krajewska M., H. G. Wang, S. Krajewski, J. M. Zapata, A. Shabaik, R. Gascoyne, J. C. Reed. Immunohistochemical analysis of in vivo patterns of expression of CPP32 (Caspase-3), a cell death protease. *Cancer Res.*57:1605-1613, 1997.
 74. Samali A., B. Zhivotovsky, D. P. Jones, S. Orrenius. Detection of pro-caspase-3 in cytosol and mitochondria of various tissues. *FEBS Lett.*431:167-169, 1998.

75. Gellerich F. N., S. Trumbeckaite, K. Hertel, S. Zierz, U. Muller-Werdan, K. Werdan, H. Redl, G. Schlag. Impaired energy metabolism in hearts of septic baboons: diminished activities of Complex I and Complex II of the mitochondrial respiratory chain. *Shock*.11:336-341, 1999.
76. Oddis C. V., M. S. Finkel. Cytokine-stimulated nitric oxide production inhibits mitochondrial activity in cardiac myocytes. *Biochem Biophys Res Commun*.213:1002-1009, 1995.
77. Yasuda S., W. Y. Lew. Angiotensin II exacerbates lipopolysaccharide-induced contractile depression in rabbit cardiac myocytes. *Am J Physiol*.276:H1442-1449, 1999.
78. Liu L., G. Azhar, W. Gao, X. Zhang, J. Y. Wei. Bcl-2 and Bax expression in adult rat hearts after coronary occlusion: age-associated differences. *Am. J. Physiol*.275:R315-322, 1998.
79. Arstall M. A., D. B. Sawyer, R. Fukazawa, R. A. Kelly. Cytokine-mediated apoptosis in cardiac myocytes: the role of inducible nitric oxide synthase induction and peroxynitrite generation. *Circ Res*.85:829-840, 1999.
80. Wang L., W. Ma, R. Markovich, J. W. Chen, P. H. Wang. Regulation of cardiomyocyte apoptotic signaling by insulin-like growth factor I. *Circ. Res*.83:516-522, 1998.
81. Wang L., W. Ma, R. Markovich, W. L. Lee, P. H. Wang. Insulin-like growth factor I modulates induction of apoptotic signaling in H9C2 cardiac muscle cells. *Endocrinology*.139:1354-1360, 1998.

82. Maulik N., S. Goswami, N. Galang, D. K. Das. Differential regulation of Bcl-2, AP-1 and NF-kappaB on cardiomyocyte apoptosis during myocardial ischemic stress adaptation. *FEBS Lett.*443:331-336, 1999.
83. Slee E., M. Harte, S. Martin. A duel to the death:activated caspases meet their substrates. *Sepsis: An Interdisciplinary Journal.*2:21-29, 1998.
84. Cook S. A., P. H. Sugden, A. Clerk. Regulation of bcl-2 family proteins during development and in response to oxidative stress in cardiac myocytes: association with changes in mitochondrial membrane potential [see comments]. *Circ Res.*85:940-949, 1999.
85. Moulding D. A., J. A. Quayle, C. A. Hart, S. W. Edwards. Mcl-1 expression in human neutrophils: regulation by cytokines and correlation with cell survival. *Blood.*92:2495-2502, 1998.
86. Krajewski S., M. Krajewska, A. Shabaik, T. Miyashita, H. G. Wang, J. C. Reed. Immunohistochemical determination of in vivo distribution of Bax, a dominant inhibitor of Bcl-2. *Am J Pathol.*145:1323-1336, 1994.
87. Murphy M. P. Nitric oxide and cell death. *Biochim Biophys Acta.*1411:401-414, 1999.
88. Xie K., S. Huang, Y. Wang, P. J. Beltran, S. H. Juang, Z. Dong, J. C. Reed, T. J. McDonnell, D. J. McConkey, I. J. Fidler. Bcl-2 protects cells from cytokine-induced nitric-oxide-dependent apoptosis. *Cancer Immunol. Immunother.*43:109-115, 1996.
89. De Vos K., V. Goossens, E. Boone, D. Vercammen, K. Vancompernelle, P. Vandenabeele, G. Haegeman, W. Fiers, J. Grooten. The 55-kDa tumor necrosis

factor receptor induces clustering of mitochondria through its membrane-proximal region. *J. Biol. Chem.* 273:9673-9680, 1998.

90. Higuchi M., B. B. Aggarwal, E. T. Yeh. Activation of CPP32-like protease in tumor necrosis factor-induced apoptosis is dependent on mitochondrial function. *J. Clin. Invest.* 99:1751-1758, 1997.
91. Shidoji Y., K. Hayashi, S. Komura, N. Ohishi, K. Yagi. Loss of molecular interaction between cytochrome c and cardiolipin due to lipid peroxidation. *Biochem Biophys Res Commun.* 264:343-347, 1999.
92. Brown G. C. Nitric oxide and mitochondrial respiration. *Biochim Biophys Acta.* 1411:351-369, 1999.
93. Uyemura S. A., S. Albuquerque, C. Curti. Energetics of heart mitochondria during acute phase of *Trypanosoma cruzi* infection in rats. *Int J Biochem Cell Biol.* 27:1183-1189, 1995.
94. Piper H. M., O. Sezer, M. Schleyer, P. Schwartz, J. F. Hutter, P. G. Spieckermann. Development of ischemia-induced damage in defined mitochondrial subpopulations. *J Mol Cell Cardiol.* 17:885-896, 1985.
95. Narula J., P. Pandey, E. Arbustini, N. Haider, N. Narula, F. D. Kolodgie, B. Dal Bello, M. J. Semigran, A. Bielsa-Masdeu, G. W. Dec, S. Israels, M. Ballester, R. Virmani, S. Saxena, S. Kharbanda. Apoptosis in heart failure: release of cytochrome c from mitochondria and activation of caspase-3 in human cardiomyopathy. *Proc Natl Acad Sci U S A.* 96:8144-8149, 1999.
96. von Harsdorf R., P. F. Li, R. Dietz. Signaling pathways in reactive oxygen species-induced cardiomyocyte apoptosis. *Circulation.* 99:2934-2941, 1999.

97. Poyton R. O., P. V. Burke. Oxygen regulated transcription of cytochrome c and cytochrome c oxidase genes in yeast. *Biochim Biophys Acta*.1101:252-256, 1992.
98. Hotchkiss R. S., I. E. Karl. Reevaluation of the role of cellular hypoxia and bioenergetic failure in sepsis. *Jama*.267:1503-1510, 1992.
99. Ince C., M. Sinaasappel. Microcirculatory oxygenation and shunting in sepsis and shock [see comments]. *Crit Care Med*.27:1369-1377, 1999.
100. Hotchkiss R. S., R. S. Rust, C. S. Dence, T. H. Wasserman, S. K. Song, D. R. Hwang, I. E. Karl, M. J. Welch. Evaluation of the role of cellular hypoxia in sepsis by the hypoxic marker [¹⁸F]fluoromisonidazole. *Am J Physiol*.261:R965-972, 1991.
101. Bobba A., A. Atlante, S. Giannattasio, G. Sgaramella, P. Calissano, E. Marra. Early release and subsequent caspase-mediated degradation of cytochrome c in apoptotic cerebellar granule cells. *FEBS Lett*.457:126-130, 1999.
102. Kovacs A., M. R. Courtois, B. Barzilai, I. E. Karl, P. A. Ludbrook, R. S. Hotchkiss. Reversal of hypocalcemia and decreased afterload in sepsis. Effect on myocardial systolic and diastolic function. *Am J Respir Crit Care Med*.158:1990-1998, 1998.
103. Korshunov S. S., B. F. Krasnikov, M. O. Pereverzev, V. P. Skulachev. The antioxidant functions of cytochrome c. *FEBS Lett*.462:192-198, 1999.
104. Vinten-Johansen J., V. H. Thourani, R. S. Ronson, J. E. Jordan, Z. Q. Zhao, M. Nakamura, D. Velez, R. A. Guyton. Broad-spectrum cardioprotection with adenosine. *Ann Thorac Surg*.68:1942-1948, 1999.

105. Stoclet J. C., B. Muller, K. Gyorgy, R. Andriantsiothaina, A. L. Kleschyov. The inducible nitric oxide synthase in vascular and cardiac tissue. *Eur J Pharmacol.*375:139-155, 1999.
106. Black S. C., J. Q. Huang, P. Rezaiefar, S. Radinovic, A. Eberhart, D. W. Nicholson, I. W. Rodger. Co-localization of the cysteine protease caspase-3 with apoptotic myocytes after in vivo myocardial ischemia and reperfusion in the rat. *J. Mol. Cell. Cardiol.*30:733-742, 1998.
107. Yaoita H., K. Ogawa, K. Maehara, Y. Maruyama. Attenuation of ischemia/reperfusion injury in rats by a caspase inhibitor. *Circulation.*97:276-281, 1998.
108. Yue T. L., C. Wang, A. M. Romanic, K. Kikly, P. Keller, W. E. DeWolf, Jr., T. K. Hart, H. C. Thomas, B. Storer, J. L. Gu, X. Wang, G. Z. Feuerstein. Staurosporine-induced apoptosis in cardiomyocytes: A potential role of caspase-3. *J. Mol. Cell. Cardiol.*30:495-507, 1998.
109. Geng Y. J., T. Azuma, J. X. Tang, J. H. Hartwig, M. Muszynski, Q. Wu, P. Libby, D. J. Kwiatkowski. Caspase-3-induced gelsolin fragmentation contributes to actin cytoskeletal collapse, nucleolysis, and apoptosis of vascular smooth muscle cells exposed to proinflammatory cytokines. *Eur J Cell Biol.*77:294-302, 1998.
110. Ing D. J., J. Zang, V. J. Dzau, K. A. Webster, N. H. Bishopric. Modulation of cytokine-induced cardiac myocyte apoptosis by nitric oxide, Bak, and Bcl-x. *Circ. Res.*84:21-33, 1999.
111. Geng Y. J., Q. Wu, M. Muszynski, G. K. Hansson, P. Libby. Apoptosis of vascular smooth muscle cells induced by in vitro stimulation with interferon-

- gamma, tumor necrosis factor-alpha, and interleukin-1 beta. *Arterioscler. Thromb. Vasc. Biol.* 16:19-27, 1996.
112. Messmer U. K., G. Winkel, V. A. Briner, J. Pfeilschifter. Glucocorticoids potentially block tumour necrosis factor-alpha- and lipopolysaccharide-induced apoptotic cell death in bovine glomerular endothelial cells upstream of caspase 3 activation. *Br J Pharmacol.* 127:1633-1640, 1999.
 113. Olivetti G., F. Quaini, R. Sala, C. Lagrasta, D. Corradi, E. Bonacina, S. R. Gambert, E. Cigola, P. Anversa. Acute myocardial infarction in humans is associated with activation of programmed myocyte cell death in the surviving portion of the heart. *J. Mol. Cell Cardiol.* 28:2005-2016, 1996.
 114. Sharov V. G., H. N. Sabbah, H. Shimoyama, A. V. Goussev, M. Lesch, S. Goldstein. Evidence of cardiocyte apoptosis in myocardium of dogs with chronic heart failure. *Am. J. Pathol.* 148:141-149, 1996.
 115. Aikawa R., I. Komuro, T. Yamazaki, Y. Zou, S. Kudoh, M. Tanaka, I. Shiojima, Y. Hiroi, Y. Yazaki. Oxidative stress activates extracellular signal-regulated kinases through Src and Ras in cultured cardiac myocytes of neonatal rats. *J Clin Invest.* 100:1813-1821, 1997.
 116. Pinsky D. J., W. Aji, M. Szabolcs, E. S. Athan, Y. Liu, Y. M. Yang, R. P. Kline, K. E. Olson, P. J. Cannon. Nitric oxide triggers programmed cell death (apoptosis) of adult rat ventricular myocytes in culture. *Am J Physiol.* 277:H1189-1199, 1999.
 117. Pulkki K. J. Cytokines and cardiomyocyte death. *Ann. Med.* 29:339-343, 1997.

118. Kawaguchi H., W. S. Shin, Y. Wang, M. Inukai, M. Kato, Y. Matsuo-Okai, A. Sakamoto, Y. Uehara, Y. Kaneda, T. Toyo-oka. In vivo gene transfection of human endothelial cell nitric oxide synthase in cardiomyocytes causes apoptosis-like cell death. Identification using Sendai virus-coated liposomes. *Circulation*.95:2441-2447, 1997.
119. Shames B. D., D. R. Meldrum, C. H. Selzman, E. J. Pulido, B. S. Cain, A. Banerjee, A. H. Harken, X. Meng. Increased levels of myocardial IkappaB-alpha protein promote tolerance to endotoxin. *Am J Physiol*.275:H1084-1091, 1998.
120. Toborek M., E. M. Blanc, S. Kaiser, M. P. Mattson, B. Hennig. Linoleic acid potentiates TNF-mediated oxidative stress, disruption of calcium homeostasis, and apoptosis of cultured vascular endothelial cells. *J. Lipid Res*.38:2155-2167, 1997.
121. Bensard D. D., A. Banerjee, R. C. McIntyre, Jr., R. L. Berens, A. H. Harken. Endotoxin disrupts beta-adrenergic signal transduction in the heart. *Arch Surg*.129:198-204; discussion 204-195, 1994.
122. Communal C., K. Singh, D. B. Sawyer, W. S. Colucci. Opposing effects of beta(1)- and beta(2)-adrenergic receptors on cardiac myocyte apoptosis : role of a pertussis toxin-sensitive G protein. *Circulation*.100:2210-2212, 1999.
123. Iwai-Kanai E., K. Hasegawa, M. Araki, T. Kakita, T. Morimoto, S. Sasayama. alpha- and beta-adrenergic pathways differentially regulate cell type-specific apoptosis in rat cardiac myocytes. *Circulation*.100:305-311, 1999.

124. Geng Y. J., Y. Ishikawa, D. E. Vatner, T. E. Wagner, S. P. Bishop, S. F. Vatner, C. J. Homcy. Apoptosis of cardiac myocytes in Gsalpha transgenic mice. *Circ. Res.* 84:34-42, 1999.
125. Wu L. L., M. S. Liu. Heart sarcolemmal Ca²⁺ transport in endotoxin shock: I. Impairment of ATP-dependent Ca²⁺ transport. *Mol Cell Biochem.* 112:125-133, 1992.
126. McConkey D. J. The role of calcium in the regulation of apoptosis. *Scanning Microsc.* 10:777-793; discussion 793-774, 1996.
127. Simms M., P. Walley, B. Munt, D. Buchowshi, K. Walley. Characterization of the pattern of septic myocardial dysfunction in mice using echocardiography. *FASEB.* J13:A109, 1999.
128. Meng X., L. Ao, D. R. Meldrum, B. S. Cain, B. D. Shames, C. H. Selzman, A. Banerjee, A. H. Harken. TNF-alpha and myocardial depression in endotoxemic rats: temporal discordance of an obligatory relationship. *Am J Physiol.* 275:R502-508, 1998.
129. Hung J., W. Y. Lew. Temporal sequence of endotoxin-induced systolic and diastolic myocardial depression in rabbits. *Am J Physiol.* 265:H810-819, 1993.
130. Adams H. R., C. R. Baxter, J. L. Parker. Reduction of intrinsic contractile reserves of the left ventricle by Escherichia coli endotoxin shock in guinea-pigs. *J Mol Cell Cardiol.* 17:575-585, 1985.
131. Herbertson M. J., H. A. Werner, K. R. Walley. Nitric oxide synthase inhibition partially prevents decreased LV contractility during endotoxemia. *Am. J. Physiol.* 270:H1979-1984, 1996.

132. MacLellan W. R., M. D. Schneider. Death by design. Programmed cell death in cardiovascular biology and disease. *Circ. Res.*81:137-144, 1997.
133. Hung W. C., L. Y. Chuang. Induction of apoptosis by sphingosine-1-phosphate in human hepatoma cells is associated with enhanced expression of bax gene product. *Biochem Biophys Res Commun.*229:11-15, 1996.
134. Yang S. L., C. Hsu, S. I. Lue, H. K. Hsu, J. Yang, M. S. Liu. Protein kinase C activity is increased in rat heart during the early hyperdynamic phase of sepsis. *Shock.*9:199-203, 1998.
135. Higuchi M., R. J. Proske, E. T. Yeh. Inhibition of mitochondrial respiratory chain complex I by TNF results in cytochrome c release, membrane permeability transition, and apoptosis. *Oncogene.*17:2515-2524, 1998.
136. Hsu C., S. L. Yang, S. P. Hsu, H. K. Hsu, M. S. Liu. Differential activation of protein kinase A in various regions of myocardium during sepsis. *J Surg Res.*71:161-165, 1997.
137. Minamikawa T., D. A. Williams, D. N. Bowser, P. Nagley. Mitochondrial permeability transition and swelling can occur reversibly without inducing cell death in intact human cells. *Exp. Cell Res.*246:26-37, 1999.